

---

# LoopRPT: Reinforcement Pre-Training for Looped Language Models

---

Guo Tang<sup>\*1</sup> Shixin Jiang<sup>\*1</sup> Heng Chang<sup>\*‡2</sup> Nuo Chen<sup>3</sup> Yuhan Li<sup>3</sup> Huiming Fan<sup>1</sup> Jia Li<sup>3</sup> Ming Liu<sup>1</sup>  
Bing Qin<sup>1</sup>

## Abstract

Looped language models (LoopLMs) perform iterative latent computation to refine internal representations, offering a promising alternative to explicit chain-of-thought (CoT) reasoning. However, existing reinforcement learning (RL) paradigms primarily target output tokens, creating a structural mismatch with looped architectures whose reasoning unfolds implicitly. In this work, we propose **LoopRPT**, a reinforcement pre-training framework tailored for LoopLMs. By reframing next-token prediction as a next-token reasoning task, LoopRPT assigns reinforcement signals directly to latent steps using an EMA teacher reference and noisy latent rollouts. This formulation enables RL to directly shape intermediate representations, compressing effective reasoning into fewer iterations. We instantiate LoopRPT on the Ouro architecture across multiple model scales. Results demonstrate that LoopRPT consistently improves per-step representation quality, achieving Pareto dominance in accuracy–computation trade-offs. Notably, significant gains on hard tokens indicate that LoopRPT enhances early-stage reasoning rather than merely encouraging premature exits. Our findings highlight reinforcement pre-training as a principled paradigm for learning efficient latent reasoning in LoopLMs.

## 1. Introduction

Modern Large Language Models (LLMs) are trained to “think” primarily through explicit text generation, such as chain-of-thought (CoT) prompting (Wei et al., 2022). While effective, this paradigm defers reasoning to post-training and often under-leverages the rich structural information available in pre-training data (Christiano et al., 2017; Wen

et al., 2025; Guo et al., 2025). In contrast, Looped Language Models (LoopLMs)—as exemplified by architectures like Ouro—utilize a parameter-shared looped backbone where internal representations are refined recurrently in latent space (Zhu et al., 2025). This allows the model to perform iterative computation, enabling deeper reasoning capabilities without a proportional increase in parameter count. As illustrated in Figure 1a, LoopLMs offer a promising alternative by compressing multi-step reasoning into latent transitions rather than consuming explicit tokens.

However, effectively incentivizing these looped structures using reinforcement learning (RL) remains a significant challenge. Traditional Reinforcement Learning with Verifiable Rewards (RLVR) paradigms primarily operate on output tokens, creating a structural mismatch with looped architectures whose reasoning unfolds implicitly (Shao et al., 2024; Wen et al., 2025). As explicitly identified in recent studies on the Ouro architecture (Zhu et al., 2025), the dynamic early-exit mechanism—which adaptively determines computation depth—introduces instability and credit assignment issues for standard RLVR alignment. This leads to a fundamental research question:

*How to incentivize LoopLMs using RL with performance gains compared to non-recursive transformer models?*

Current RLVR tasks rely on sparse rewards derived from final output tokens, which are insufficient for the dense, multi-step latent reasoning required by LoopLMs. Recently, **Reinforcement Pre-Training (RPT)** has emerged as a new scaling paradigm, reframing next-token prediction as a reasoning task (Hatamizadeh et al., 2025; Dong et al., 2025). By treating internal computation as an exploratory action and assigning rewards based on the predictive gain for future tokens, RPT enables the leveraging of vast amounts of text data for general-purpose RL. This transition from sparse output feedback to dense, self-supervised next-token reasoning signals provides a clear path toward effectively training looped architectures.

In this work, we make the first attempt to unify looped architectures with the RPT paradigm. Our initial analysis, shown in Figure 1b, reveals that LoopLMs are naturally “reasoning-friendly” for next-token tasks. Vanilla LLMs,

---

<sup>\*</sup>Equal contribution <sup>‡</sup>Project lead <sup>1</sup>Harbin Institute of Technology, Harbin, China <sup>2</sup>Tsinghua University, Beijing, China <sup>3</sup>The Hong Kong University of Science and Technology, Guangzhou, China. Correspondence to: Ming Liu <mliu@ir.hit.edu.cn>.

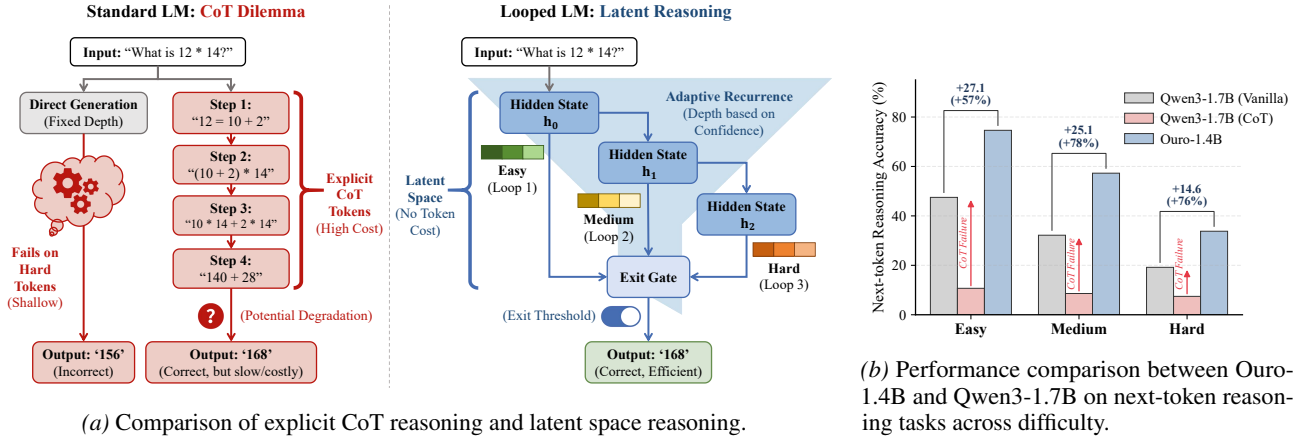


Figure 1. **Motivation for LoopRPT.** (a) Standard LLMs rely on explicit chain-of-thought tokens for reasoning, leading to increased token usage, whereas looped language models compress multi-step reasoning into latent space. (b) Looped language models achieve higher accuracy than standard LLMs on next-token reasoning tasks across difficulty levels.

lacking specialized training for CoT-based next-token reasoning tasks, exhibit significant performance degradation. We observe that looped models consistently achieve higher accuracy than standard LLMs across varying difficulty levels. This suggests that the superior knowledge manipulation capabilities of LoopLMs can be systematically unlocked by an RL algorithm designed specifically for latent recurrence.

To fill this gap, we propose **LoopRPT**, a **Reinforcement Pre-Training Framework** tailored for **Looped LMs**. Built upon the next-token reasoning task, LoopRPT assigns reinforcement signals directly to latent reasoning steps. The framework incorporates three key innovations: (i) an **entropy-based selector** that identifies "hard tokens" where reasoning is most beneficial (Wang et al., 2025), (ii) **step-wise rewards** computed against a dynamic EMA teacher to shape intermediate representations (Tavainen & Valpola, 2017; Hatamizadeh et al., 2025), and (iii) **noisy latent rollouts** to jointly optimize the exit policy and backbone representations. By combining accuracy gains with a difficulty-aware time penalty, LoopRPT encourages early effective exits without sacrificing correctness on challenging tokens.

We conduct extensive experiments on Ouro-1.4B and Ouro-2.6B using the OMNI-MATH (Gao et al., 2024a) and general reasoning datasets. Our results demonstrate that LoopRPT consistently improves per-step representation quality and achieves a superior accuracy-computation trade-off. Specifically, LoopRPT significantly reduces average computation steps while maintaining or improving performance on hard tokens. These gains transfer to downstream benchmarks, with notable improvements in GSM8K (Cobbe et al., 2021), MBPP (Austin et al., 2021), and HumanEval (Chen et al., 2021).

Our primary contributions are summarized as follows:

- We introduce **LoopRPT**, the first framework to apply the Reinforcement Pre-Training paradigm to Looped LMs, addressing the mismatch between latent reasoning and sparse token-level rewards.
- We design a novel **step-wise reinforcement objective** utilizing an EMA teacher and noisy latent rollouts to provide dense supervision over internal recurrent transitions.
- Empirical results show that LoopRPT achieves Pareto dominance in accuracy-computation trade-offs across multiple scales, outperforming both vanilla looped models and standard LLMs with explicit CoT.

## 2. Preliminaries

**Looped Language Models (LoopLMs)** Unlike standard transformers, LoopLMs refine internal representations through iterative latent computation. Given context  $x_{<t}$ , the model updates a latent state  $\mathbf{h}^{(k)}$  via a parameter-shared backbone  $f_\theta$ :

$$\mathbf{h}^{(k+1)} = f_\theta(\mathbf{h}^{(k)}, x_{<t}), \quad k = 0, \dots, K - 1, \quad (1)$$

The next-token distribution is then derived from the final state:  $p_\theta(x_t | x_{<t}) = g_\theta(\mathbf{h}^{(K)})$ , where  $g_\theta$  represents an LM head. This architecture enables multi-step reasoning in latent space without the cost of emitting intermediate tokens.

**Standard Next-Token Prediction (NTP)** remains the dominant objective, maximizing the log-likelihood:  $\mathcal{L}_{\text{NTP}}(\theta) = -\sum \log p_\theta(x_t | x_{<t})$ . However, NTP treats predictions independently and fails to explicitly model the latent reasoning processes required for difficult tokens.

**Reinforcement Pre-Training (RPT)** reframes prediction as a reasoning task. The model samples an output

$o_t \sim \pi_\theta$  and receives a verifiable reward  $r(o_t, x_t)$  based on the ground-truth continuation. The objective maximizes the expected reward over the corpus:  $\mathcal{J}_{\text{RPT}}(\theta) = \mathbb{E}_{x_{<t}} \mathbb{E}_{o_t \sim \pi_\theta(\cdot | x_{<t})} [r(o_t, x_t)]$ . By leveraging intrinsic corpus rewards, RPT scales reinforcement learning to large datasets, incentivizing next-token reasoning over simple likelihood maximization.

### 3. Method

In the RLVR paradigm, rewards are typically sparse as they are derived solely from feedback on final answer tokens. For looped LMs that perform multi-step reasoning in latent space, this sparsity exacerbates the credit assignment challenge across intermediate iterations. To address this, we introduce dense step-wise reward signals, focusing them on challenging next-token predictions, which enables looped LMs to improve intermediate reasoning capabilities and learn an adaptive exit policy.

Specifically, LoopRPT is a reinforcement pre-training framework tailored to looped LMs, where multi-step computation unfolds in latent space and an exit mechanism determines how many recurrent iterations are used for each token. As illustrated in Fig. 2, LoopRPT (i) selects *hard* next-token prediction instances via entropy, (ii) defines a *step-wise* reward on latent iterations relative to an EMA teacher, and (iii) jointly optimizes the exit policy and intermediate representations using noisy latent rollouts and step-weighted next-token learning.<sup>1</sup>

#### 3.1. Looped LM with an exit-step distribution

According to Sec. 2, each latent step produces next-token logits and a scalar exit-gate logit  $a^{(k)}$ , converted to an exit probability  $\lambda^{(k)} = \sigma(a^{(k)})$ . Following Ouro’s early-exit mechanism (Zhu et al., 2025), we define a survival probability  $s^{(1)} = 1$  and update

$$\pi_\theta(k) = \begin{cases} \lambda^{(k)} s^{(k)}, & k < K, \\ s^{(K)}, & k = K, \end{cases} \quad (2)$$

$$s^{(k+1)} = s^{(k)} (1 - \lambda^{(k)}) \quad (k < K), \quad (3)$$

where the last step absorbs the remaining probability mass, ensuring  $\sum_{k=1}^K \pi_\theta(k) = 1$  exactly. We compute the CDF  $\Pi(k) = \sum_{j < k} \pi_\theta(j)$  and determine the threshold exit step  $t(\tau) = \min\{k : \Pi(k) \geq \tau\}$ . For numerical robustness, if no step satisfies  $\Pi(k) \geq \tau$  (e.g., due to finite precision), we set  $t(\tau) = K$ .

<sup>1</sup>Full training algorithms are provided in App. B.

#### 3.2. Entropy-based hard-token selection

Applying reinforcement learning uniformly to all tokens is inefficient because most tokens are easy and contribute weak learning signals. LoopRPT therefore trains primarily on *hard* next-token instances identified by teacher uncertainty.<sup>2</sup> Concretely, for each position  $t$  in a sequence we compute the teacher’s next-token distribution and entropy

$$H_t = - \sum_v p_{\bar{\theta}}(v | x_{<t}) \log p_{\bar{\theta}}(v | x_{<t}), \quad (4)$$

and select a top fraction of positions (top- $\rho\%$ ) within each example as hard tokens.<sup>3</sup> All losses in Sec. 3.3–3.4 are applied only on the selected positions.

#### 3.3. Step-wise rewards with an EMA teacher

In order to provide a dense credit assignment per-step anchored by a stable moving reference (Hatamizadeh et al., 2025), LoopRPT assigns reinforcement signals *directly to latent reasoning steps* and maintains an EMA teacher  $\bar{\theta}$ .  $\bar{\theta}$  tracks student parameters  $\theta$  and serves as a dynamic reference for both exiting and reward baselines.

**Teacher reference step.** For each token, we compute the teacher’s exit distribution  $\pi_{\bar{\theta}}$  and define the teacher reference step  $t_{\text{ref}} = \min\{k : \sum_{j < k} \pi_{\bar{\theta}}(j) \geq \tau\}$ . Intuitively,  $t_{\text{ref}}$  represents the teacher’s notion of sufficient computation under the current exit threshold.

**Accuracy gain.** Let  $\ell_\theta^{(k)} = \log p_\theta(x_t | x_{<t}; \mathbf{h}^{(k)}) \in \mathbb{R}^{B \times (S-1)}$  denote the student log-probability of the ground-truth next token when read out from step  $k$ . We take the teacher log-probability at the reference step as a per-token baseline,

$$b_{\text{ref}} = \ell_{\bar{\theta}}^{(t_{\text{ref}})} \in \mathbb{R}^{B \times (S-1)}. \quad (5)$$

The step-wise accuracy gain is

$$\Delta_{\text{acc}}(k) = \ell_\theta^{(k)} - b_{\text{ref}}. \quad (6)$$

**Difficulty-aware time penalty.** To encourage earlier *effective* exits without forcing premature termination on difficult tokens, we penalize excessive computation relative to the teacher reference step:

$$C(k) = \lambda_t (k - t_{\text{ref}}). \quad (7)$$

Here  $\lambda_t$  is a token-dependent penalty weight derived from teacher uncertainty at the reference step. Specifically, we compute the entropy  $H_t$  at the teacher’s reference step distribution, normalize  $H_t$  by  $\log |\mathcal{V}|$  and clamp it to obtain a

<sup>2</sup>We provide theoretical analysis in App. A.1.

<sup>3</sup>Details are deferred to App. C.

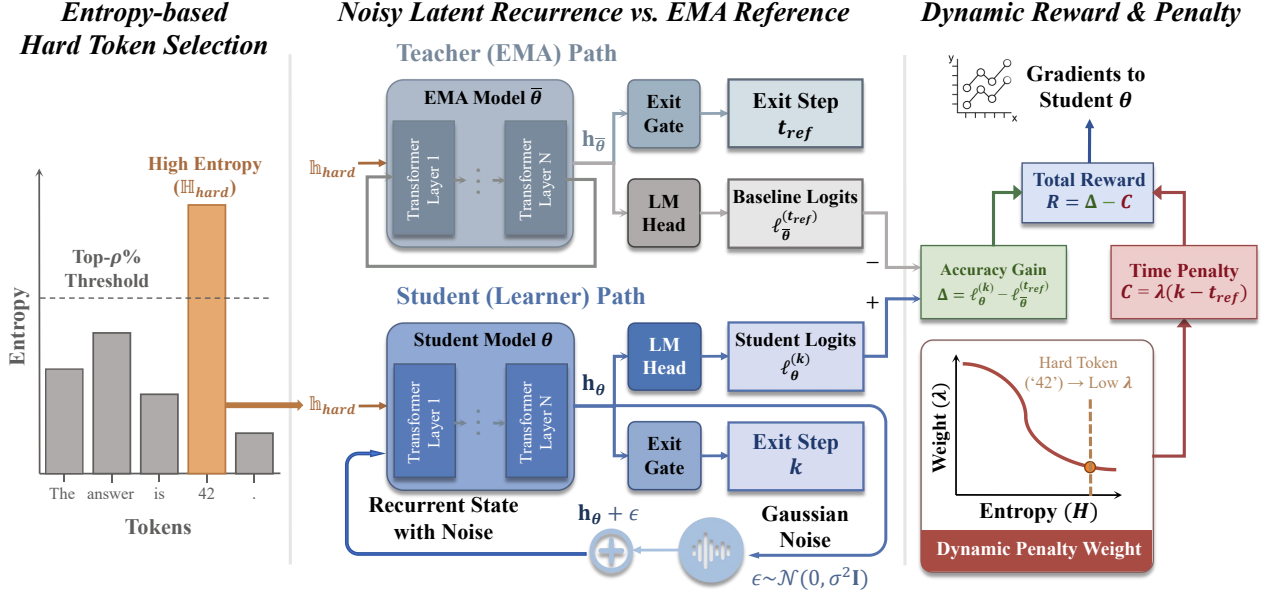


Figure 2. Overview of **LoopRPT**. Given a looped architecture with latent recurrence, LoopRPT assigns reinforcement signals directly to latent reasoning steps. An entropy-based selector identifies hard tokens, for which a student model is trained against an EMA teacher via step-wise rewards. The total reward combines an accuracy gain relative to the teacher baseline and a dynamic time penalty, enabling reinforcement learning to shape intermediate representations and encourage earlier effective exits without premature termination.

difficulty score  $d_t = \text{Clamp}(H_t / \log |\mathcal{V}|, 0, 1)$ . We introduce the base coefficient  $\lambda_{\text{base}}$  and the scaling coefficient  $\lambda_{\text{scale}}$ , thus  $\lambda_t$  is defined as

$$\lambda_t = \lambda_{\text{base}} \left( 1 + \lambda_{\text{scale}} (1 - d_t) \right), \quad (8)$$

so that easier tokens (lower entropy) incur larger time penalties, while harder tokens are penalized less.

**Total step-wise reward.** Combining the above, LoopRPT defines a reward for each latent step:

$$R(k) = \Delta_{\text{acc}}(k) - C(k). \quad (9)$$

This reward provides dense supervision over latent iterations, shaping intermediate representations and aligning them with early exiting (Fig. 2).

Finally, we compute a per-token *step advantage* by normalizing  $R(k)$  across steps  $k = 1, \dots, K$ :

$$\hat{A}(k) = \frac{R(k) - \mu_R}{\sigma_R + \epsilon}, \quad \mu_R = \frac{1}{K} \sum_{j=1}^K R(j), \quad (10)$$

which will be used to emphasize beneficial latent steps in the representation learning objective.

### 3.4. Joint optimization via noisy latent rollouts

LoopRPT jointly trains (i) the *exit policy* induced by the gate distribution  $\pi_\theta$  and (ii) the *backbone* representations  $\{\mathbf{h}^{(k)}\}$  that support accurate prediction at early steps.

**Noisy latent rollouts for the exit policy.** As LoopLM reasoning is implicit in latent space, we obtain on-policy variability by injecting Gaussian noise into the recurrent hidden states.<sup>4</sup> For each selected token, we draw  $G$  rollouts and perturb the latent states during recurrence:

$$\mathbf{h}^{(k)} \leftarrow \mathbf{h}^{(k)} + \boldsymbol{\epsilon}^{(k)}, \quad \boldsymbol{\epsilon}^{(k)} \sim \mathcal{N}(0, \sigma^2 \mathbf{I}), \quad (11)$$

yielding a rollout-specific exit distribution  $\pi_\theta^{(g)}(\cdot)$ . We then sample an exit step  $t^{(g)} \sim \pi_\theta^{(g)}$  and define the rollout reward by indexing the step-wise reward table in Eq. (9),  $r^{(g)} = R(t^{(g)})$ .

To stabilize policy learning, we use group-wise normalization across the  $G$  rollouts for the same input token:

$$A^{(g)} = \frac{r^{(g)} - \text{mean}_g[r^{(g)}]}{\text{std}_g[r^{(g)}] + \epsilon}. \quad (12)$$

The policy-gradient loss is

$$\mathcal{L}_{\text{PG}} = -\mathbb{E}_g [A^{(g)} \log \pi_\theta^{(g)}(t^{(g)})], \quad (13)$$

applied only on the selected hard-token positions.

**Step-weighted representation learning.** In addition to improving the exit policy, LoopRPT explicitly strengthens intermediate representations so that early latent steps can predict the correct token. Using a deterministic (noise-free)

<sup>4</sup>We provide theoretical analysis in App. A.2.

forward pass, we compute per-step log-probabilities  $\ell_\theta^{(k)}$  and the (noise-free) exit distribution  $\pi_\theta(k)$ . We then optimize a step-weighted next-token objective:

$$\mathcal{L}_{\text{rep}} = - \sum_{k=1}^K w_k \ell_\theta^{(k)}, \quad (14)$$

$$w_k = \pi_\theta(k) \left( 1 + \text{ReLU}(\hat{A}(k)) \right). \quad (15)$$

The  $\pi_\theta(k)$  term emphasizes steps the model is likely to exit from, while the advantage shaping term focuses learning on steps that yield higher rewards under Eq. (9).

**Regularization and total objective.** We add an entropy bonus on the exit distribution to prevent early collapse,  $\mathcal{L}_{\text{ent}} = -\mathbb{E}[\sum_k \pi_\theta(k) \log(\pi_\theta(k))]$ , and a KL-style trust-region penalty to the EMA teacher based on a token-level surrogate computed from teacher and student step-wise log-probabilities.<sup>5</sup> The final training loss is

$$\mathcal{L} = \alpha \mathcal{L}_{\text{PG}} + \beta \mathcal{L}_{\text{rep}} + \gamma \mathcal{L}_{\text{ent}} + \delta \mathcal{L}_{\text{KL}}. \quad (16)$$

After each update to  $\theta$ , we update the EMA teacher parameters  $\hat{\theta}$ .<sup>6</sup>

## 4. Experimental Setup

### 4.1. Training Configuration

We use OMNI-MATH (Gao et al., 2024a) as the training data. OMNI-MATH contains 4,428 competition-level mathematical problems paired with solutions, among which 200 examples are held out as the validation set. We first conduct experiments on Ouro-1.4B and then scale up to Ouro-2.6B. Both the teacher model and the student model are initialized from the same base model. The teacher parameters are maintained as an exponential moving average of the current student parameters (momentum 0.995), providing a stable reference for generating outputs, while the student model is updated via backpropagation. For token-level updates, we treat the teacher model as the entropy proxy and compute token-level entropy based on its output distribution. We then construct an entropy mask to suppress gradient updates on low-entropy tokens (Wang et al., 2025).<sup>7</sup>

### 4.2. Evaluation Setting

**Language modeling.** Following RPT (Dong et al., 2025), we evaluate the performance on the held-out validation set of 200 examples from OMNI-MATH. We bucket tokens by their entropy and report performance on easy/medium/hard

<sup>5</sup>Details are provided in App. D.

<sup>6</sup>We provide theoretical analysis in App. A.3.

<sup>7</sup>Full hyperparameters and training details are deferred to Appendix F (Table 5).

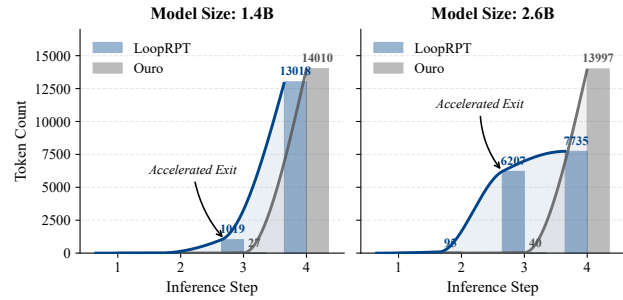


Figure 3. Distribution of exit steps on MMLU benchmark. LoopRPT increases the proportion of tokens exiting at earlier iterations while maintaining the dominant final-step exits.

splits, defined by thresholds 0.5, 1.0 and 1.5, respectively. For the Ouro models, we adopt the corresponding base model as an entropy proxy and evaluate performance under two inference settings: maximum-loop execution and adaptive early exit. We also evaluate the non-loop Qwen3-1.7B under two settings: the vanilla mode that performs NTP directly, and the CoT mode that first generates a chain-of-thought and then performs NTP.

**End tasks.** We evaluate zero-shot performance on MMLU (Hendrycks et al., 2021), MMLU-Pro (Wang et al., 2024), BBH (Suzgun et al., 2023), ARC-C (Clark et al., 2018), HellaSwag (Zellers et al., 2019), Winogrande (Sakaguchi et al., 2021), GSM8K (Cobbe et al., 2021), MBPP (Austin et al., 2021), MBPP+ (Liu et al., 2023), HumanEval (Chen et al., 2021), and HumanEval+ (Liu et al., 2023). Following Ouro (Zhu et al., 2025), all evaluations were conducted using lm-eval-harness (Gao et al., 2024b) and evalplus (Liu et al., 2023).<sup>8</sup>

## 5. Experimental Results

### 5.1. Main Results

**Next-token Reasoning (NTR).** Table 1 shows that LoopRPT consistently improves accuracy and efficiency across all scales. On Ouro-2.6B, LoopRPT boosts Hard Peak accuracy by +3.58 while reducing average steps from 3.51 to 2.28. While explicit CoT prompting on Qwen3-1.7B severely degrades performance, LoopRPT successfully compresses effective computation into fewer latent iterations without sacrificing correctness.

**Downstream Benchmarks.** As summarized in Tables 2 and 3, LoopRPT delivers consistent gains over Ouro, particularly in coding (MBPP+ +2.91) and mathematical reasoning. At the 2.6B scale, GSM8K accuracy increases from 81.76 to 85.36, alongside improvements in HumanEval+, indicating

<sup>8</sup>Detailed evaluation settings and metrics are provided in Appendix F (Table 6).

## LoopRPT: Reinforcement Pre-Training for Looped Language Models

Table 1. Performance comparison on next-token reasoning task across three difficulty levels. *Peak* indicates reasoning up to the maximum latent loops ( $K = 4$ ), while *Adap.* indicates adaptive early exiting. Subscripts indicate improvement (+) or degradation (−) compared to baseline.

Model	Method	Easy		Medium		Hard	
		Acc (↑)	Avg step (↓)	Acc (↑)	Avg step (↓)	Acc (↑)	Avg step (↓)
Qwen3-1.7B	Vanilla	47.49	–	32.18	–	19.19	–
	+CoT	10.70 <sub>−36.79</sub>	–	8.60 <sub>−23.58</sub>	–	7.44 <sub>−11.75</sub>	–
Ouro-1.4B	Peak	74.62	4.00	57.28	4.00	33.79	4.00
	<b>+LoopRPT</b>	<b>75.38</b> <sub>+0.76</sub>	4.00	<b>58.29</b> <sub>+1.01</sub>	4.00	<b>34.74</b> <sub>+0.95</sub>	4.00
	Adap.	74.40	3.34	57.20	3.53	33.91	3.75
	<b>+LoopRPT</b>	<b>75.00</b> <sub>+0.60</sub>	<b>2.50</b> <sub>−0.84</sub>	<b>57.72</b> <sub>+0.52</sub>	<b>2.81</b> <sub>−0.72</sub>	<b>34.82</b> <sub>+0.91</sub>	<b>3.07</b> <sub>−0.68</sub>
Ouro-2.6B	Peak	74.33	4.00	57.19	4.00	34.52	4.00
	<b>+LoopRPT</b>	<b>76.89</b> <sub>+2.56</sub>	4.00	<b>61.15</b> <sub>+3.96</sub>	4.00	<b>38.10</b> <sub>+3.58</sub>	4.00
	Adap.	74.51	3.24	57.35	3.35	34.35	3.51
	<b>+LoopRPT</b>	<b>76.07</b> <sub>+1.56</sub>	<b>2.05</b> <sub>−1.19</sub>	<b>60.21</b> <sub>+2.86</sub>	<b>2.18</b> <sub>−1.17</sub>	<b>37.24</b> <sub>+2.89</sub>	<b>2.28</b> <sub>−1.23</sub>

Table 2. Comparison of 1.4B LoopLM model with 1-4B parameter baselines. Results for vanilla LLMs are taken from (Zhu et al., 2025), with Ouro results obtained via our reimplementation. The best score is **bolded**, and the second-best is underlined. Subscripts indicate LoopRPT’s improvement over Ouro baseline.

Benchmark	Gemma3 1B	Llama3.2 1.2B	Qwen2.5 1.5B	Qwen3 1.7B	Qwen2.5 3B	Llama3.2 3B	Qwen3 4B	Gemma3 4B	Ouro 1.4B	<b>LoopRPT 1.4B</b>
<i>General Tasks</i>										
MMLU	39.85	45.46	60.99	62.46	65.62	59.69	<b>73.19</b>	58.37	67.35	<u>67.62</u> <sub>+0.27</sub>
MMLU-Pro	11.31	11.80	29.11	37.27	37.87	33.34	<b>51.40</b>	34.61	48.64	<u>49.21</u> <sub>+0.57</sub>
BBH	30.26	30.72	43.66	53.51	55.37	39.45	<u>70.95</u>	66.32	70.97	<b>71.37</b> <sub>+0.40</sub>
ARC-C	39.25	41.98	54.44	55.72	55.46	52.47	<b>63.65</b>	60.92	60.95	<u>61.10</u> <sub>+0.15</sub>
HellaSwag	56.12	59.35	67.73	67.09	74.54	73.09	<b>75.66</b>	<u>75.58</u>	74.30	<u>74.93</u> <sub>+0.63</sub>
Winogrande	58.72	62.75	66.77	66.30	70.17	69.14	71.19	71.07	<u>71.67</u>	<b>71.98</b> <sub>+0.31</sub>
<i>Math &amp; Coding Tasks</i>										
GSM8K	2.05	7.05	60.73	70.28	74.60	67.20	72.86	68.69	<u>78.17</u>	<b>78.92</b> <sub>+0.75</sub>
HumanEval	6.70	19.50	52.40	66.50	68.90	29.90	<b>77.40</b>	34.80	69.47	<u>69.51</u> <sub>+0.04</sub>
HumanEval+	5.50	17.40	46.30	59.80	62.20	26.20	<b>70.70</b>	29.30	67.01	<u>67.07</u> <sub>+0.06</sub>
MBPP	12.40	35.70	60.30	68.00	63.00	50.30	<b>78.80</b>	60.60	73.02	<u>75.40</u> <sub>+2.38</sub>
MBPP+	10.10	29.10	50.00	58.50	54.20	39.70	<b>65.90</b>	51.10	60.85	<u>63.76</u> <sub>+2.91</sub>

that reinforcement pre-training on hard instances effectively transfers to complex program synthesis.

**Exit Dynamics.** LoopRPT substantially strengthens adaptive exiting by increasing early-step exits while maintaining final-step dominance (Fig. 3). At larger scales, the mechanism becomes more aggressive, with a notable shift towards step-3 exits. This reflects improved confidence calibration and earlier latent convergence, aligning with the accuracy–compute Pareto dominance observed in NTR.

### 5.2. Ablation Study

Table 4 ablates key design choices of LoopRPT on Ouro-1.4B across *Hard* and *Overall* splits. Overall, removing any component degrades accuracy or efficiency, confirming that LoopRPT relies on multiple complementary ingredients.

**Stabilization and trajectory diversity.** Disabling Gaussian noise reduces accuracy and increases average exit steps, sug-

gesting that stochastic latent rollouts facilitate exploration and earlier latent convergence. Similarly, removing policy-gradient and KL stabilizers leads to significant performance drops and increased latency under adaptive inference, highlighting their importance for stable on-policy learning and calibrated early exiting.

**Representation shaping and efficiency.** Removing  $\mathcal{L}_{\text{rep}} + \mathcal{L}_{\text{ent}}$  yields the largest degradation in both accuracy and efficiency, underscoring that representation regularization and entropy shaping are vital for learning effective latent transitions. While disabling token selection slightly reduces steps, it notably hurts Hard-split accuracy, proving that hard-token updates preferentially allocate capacity to difficult reasoning tasks. Finally, removing the time penalty modestly hurts accuracy while consistently increasing average steps, confirming its role in explicitly incentivizing early exit and improving the accuracy–compute trade-off.

Table 3. Comparison of 2.6B LoopLM with 3-12B parameter baselines. Results for vanilla LLMs are taken from (Zhu et al., 2025), with Ouro results obtained via our reimplemention. Best in **bold**, second best underlined. Subscripts indicate LoopRPT’s improvement over Ouro baseline.

Benchmark	Gemma3 3B	Llama3.2 3B	Qwen2.5 4B	Qwen3 4B	Qwen2.5 7B	Llama3.1 8B	Qwen3 8B	Gemma3 12B	Ouro 2.6B	<b>LoopRPT 2.6B</b>
<i>General Tasks</i>										
MMLU	65.62	59.69	73.19	58.37	<u>74.20</u>	73.02	<b>76.63</b>	72.14	73.85	73.91 <sub>+0.06</sub>
MMLU-Pro	37.87	33.34	51.40	34.61	<u>43.55</u>	43.24	<u>53.72</u>	49.21	54.07	<b>54.19</b> <sub>+0.12</sub>
BBH	55.37	39.45	71.14	66.32	53.72	71.56	<u>77.65</u>	<b>78.41</b>	77.98	<u>78.24</u> <sub>+0.26</sub>
ARC-C	55.46	52.47	63.65	60.75	63.65	60.75	66.10	<b>72.44</b>	66.12	<u>66.89</u> <sub>+0.77</sub>
HellaSwag	74.54	73.09	75.66	75.58	79.98	<u>81.97</u>	79.60	<b>83.68</b>	79.28	80.03 <sub>+0.75</sub>
Winogrande	70.17	69.14	71.19	71.27	76.48	<u>77.11</u>	76.80	<b>77.74</b>	75.85	76.47 <sub>+0.62</sub>
<i>Math &amp; Coding Tasks</i>										
GSM8K	74.60	67.20	72.86	68.69	81.50	78.17	<u>83.09</u>	77.18	81.76	<b>85.36</b> <sub>+3.60</sub>
HumanEval	68.90	29.90	77.70	34.80	<u>79.30</u>	38.40	<b>84.80</b>	46.30	75.02	76.83 <sub>+1.81</sub>
HumanEval+	62.20	26.20	70.70	29.30	<u>70.60</u>	31.10	<b>75.30</b>	37.20	70.13	<u>71.95</u> <sub>+1.82</sub>
MBPP	63.00	50.30	<u>78.80</u>	60.60	73.80	62.40	<b>79.00</b>	73.50	77.10	<u>77.24</u> <sub>+0.14</sub>
MBPP+	54.20	39.70	65.90	51.10	63.50	51.60	<b>67.90</b>	<u>66.10</u>	64.81	65.08 <sub>+0.27</sub>

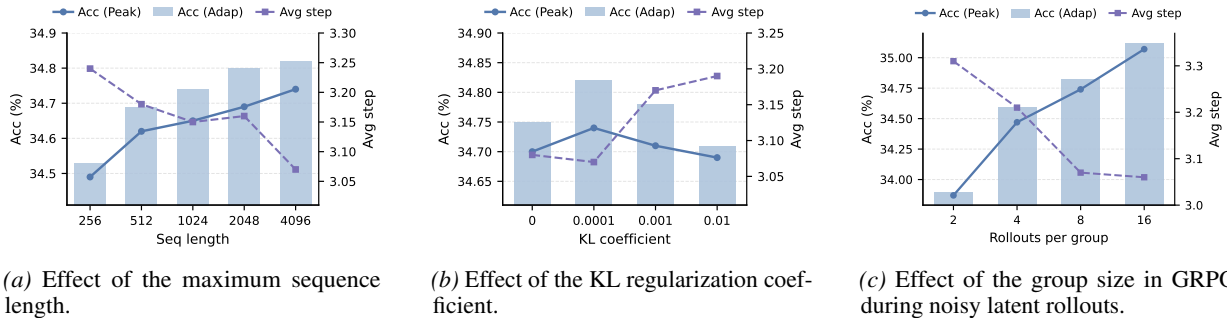


Figure 4. Sensitivity analysis of LoopRPT hyperparameters on the next-token reasoning task. All results are reported on the *hard* split, showing accuracy and average exit steps under different settings.

Table 4. Ablation study of LoopRPT-1.4B. Overall represents the average of three difficulty levels under next-token reasoning task.

Varies	Hard			Overall		
	Peak	Adap.	Avg Step	Peak	Adap.	Avg Step
<b>LoopRPT</b>	<b>34.74</b>	<b>34.82</b>	<b>3.07</b>	<b>56.14</b>	<b>55.85</b>	<b>2.79</b>
w/o Gaussian Noise	34.69	34.76	3.29 <sub>(↑)</sub>	55.86	55.57	3.17 <sub>(↑)</sub>
w/o $\mathcal{L}_{PG} + \mathcal{L}_{KL}$	34.59	34.17	3.28 <sub>(↑)</sub>	55.89	55.51	3.14 <sub>(↑)</sub>
w/o $\mathcal{L}_{rep} + \mathcal{L}_{ent}$	34.02	33.75	3.46 <sub>(↑)</sub>	55.52	55.19	3.24 <sub>(↑)</sub>
w/o Token Selection	34.60	34.52	2.89 <sub>(↓)</sub>	55.76	55.41	2.49 <sub>(↓)</sub>
w/o Time Penalty	34.57	34.80	3.30 <sub>(↑)</sub>	55.94	55.78	3.19 <sub>(↑)</sub>

## 6. Analysis and Discussion

### 6.1. Hyperparameter Sensitivity

LoopRPT exhibits low sensitivity to key hyperparameters and follows a predictable accuracy–compute trade-off. Increasing the maximum sequence length (see Fig. 4a) consistently improves both *Peak* and *Adap.* accuracy, while the average exit step slightly decreases or saturates, suggesting that longer context helps latent computation converge earlier. The KL regularization coefficient (Fig. 4b) shows a mild sweet spot: moderate KL improves *Adap.* perfor-

mance, whereas overly strong KL tends to reduce gains and yields more conservative exiting (higher average steps), consistent with over-constraining on-policy updates. Finally, enlarging the GRPO group size (Fig. 4c) improves accuracy and reduces average steps, indicating that better group-wise advantage estimates strengthen both learning signal and early-exit calibration, with diminishing returns at larger group sizes.

### 6.2. Analysis of Latent Reasoning

To better understand how LoopRPT improves the accuracy–computation trade-off, we analyze the latent reasoning dynamics of LoopLMs at the level of intermediate computation steps. Fig. 5 presents the accuracy–computation Pareto curves under varying exit thresholds. Across three difficulty buckets, LoopRPT consistently achieves higher accuracy with fewer average computation steps compared to the baseline Ouro model. Notably, this Pareto dominance holds across model scales, indicating that the gains introduced by LoopRPT are not tied to a specific parameter regime.

To uncover the mechanism behind this improvement, Fig. 6

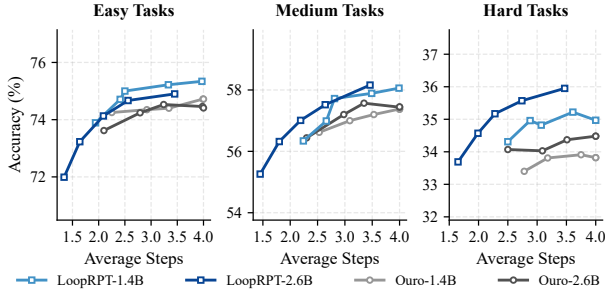


Figure 5. Accuracy-computation trade-offs across difficulty buckets. LoopRPT enhances next-token reasoning accuracy with reduced loop cycles.

reports per-step next-token prediction accuracy obtained from intermediate hidden states within a single forward pass. We observe that LoopRPT improves prediction accuracy at every latent step, with particularly pronounced gains at early steps. This effect is most evident for hard tokens, where LoopRPT significantly boosts step-1 and step-2 accuracy.

These results suggest that LoopRPT does not merely encourage earlier exiting, but fundamentally enhances the quality of intermediate representations. By shaping latent reasoning through reinforcement pre-training, LoopRPT compresses effective computation into fewer steps while preserving or improving predictive performance.

### 6.3. Forced-depth Evaluation

We set the exit threshold to 1.0 and vary the latent steps to evaluate performance under compulsory computation. As shown in Fig. 7, forced-depth accuracy is not guaranteed to improve monotonically as depth increases, and may even degrade for Medium and Hard buckets. This behavior is expected for looped models: later latent steps are not explicitly optimized to monotonically refine token-level cross-entropy, and additional iterations can introduce distributional shifts or over-updating of latent representations when the model is forced to continue reasoning. Consequently, forced-depth evaluation measures the behavior under compulsory computation, rather than the intrinsic quality of intermediate representations.

Importantly, LoopRPT consistently outperforms the baseline across all buckets and depths, indicating that reinforcement pre-training improves robustness even under forced computation.

## 7. Related Work

**Reinforcement learning for (pre-)training LMs.** Modern RL-based post-training for LMs is often instantiated as RL from preference feedback, where a reward model (or an implicit reward) is optimized with policy-gradient style up-

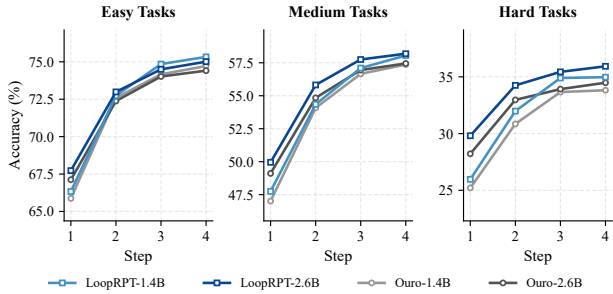


Figure 6. Per-step next-token reasoning accuracy across difficulty buckets.

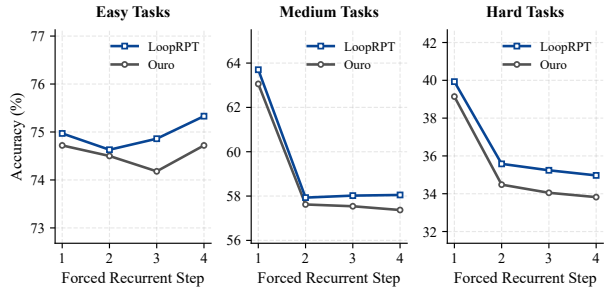


Figure 7. Forced-depth evaluation across difficulty buckets.

dates such as TRPO/PPO (Schulman et al., 2015; 2017) and human preference supervision (Christiano et al., 2017; Stiennon et al., 2020; Ouyang et al., 2022). Subsequent work reduces reliance on human labels by leveraging AI feedback and rule-based supervision, e.g., Constitutional AI / RLAIF (Bai et al., 2022), and broadens the algorithmic toolkit beyond reward-model RLHF via direct/implicit preference optimization (Rafailov et al., 2023; Ethayarajh et al., 2024; Hong et al., 2024) and their extensions and surveys (Xiao et al., 2025; Jiang et al., 2025; Cen et al., 2025). In parallel, RLVR exploit programmatic or checker-based supervision to improve reasoning without a learned reward model (Wen et al., 2025; Guo et al., 2025; Shao et al., 2024), but are typically applied as task-specific post-training due to limited availability of verifiable supervision at scale. Reinforcement Pre-Training (RPT) reframes next-token prediction itself as a verifiable RL objective, enabling RL signals to be derived directly from the pre-training corpus (Dong et al., 2025; Hatamizadeh et al., 2025). Our work follows this emerging direction and addresses a key bottleneck for RL pre-training: token-level feedback is naturally sparse and dominated by easy transitions. By concentrating dense updates on hard next-token instances (Wang et al., 2025), we improve both token-level reasoning and downstream transfer while preserving stable training dynamics.

**Looped language models and adaptive depth.** A long line of work explores recurrence and adaptive computation

in neural sequence models. Early approaches introduce dynamic halting and step allocation, such as ACT (Graves, 2016) and Universal Transformers (Dehghani et al., 2019), later extended with sparse/shared-depth variants (Tan et al., 2023) and learned pondering mechanisms (Banino et al., 2021). Complementary to within-token recurrence, recurrence over segments and explicit memory has been studied for long-context modeling, e.g., Transformer-XL (Dai et al., 2019), Compressive Transformers (Rae et al., 2019) and Recurrent Memory Transformers (Bulatov et al., 2022). Another related line is dynamic-depth inference via early exiting or layer-wise halting (Xin et al., 2020; Zhou et al., 2020; Xu & McAuley, 2023; Bajpai & Hanawal, 2025), and more recent efforts allocate compute non-uniformly across tokens/layers (Raposo et al., 2024; Chen et al., 2025). Closest to our setting are Looped/Depth-recurrent LMs that explicitly build iterative latent computation into the model, enabling adaptive early exit at test time (Zhu et al., 2025; Wu et al., 2025; Li et al., 2025; McLeish et al., 2025), as well as related latent-pondering pretraining schemes (Zeng et al., 2025). Our work is positioned at the intersection: we leverage LoopLMs as the computational substrate, and contribute an RL pre-training recipe that strengthens token-level reasoning and calibrates early-exit behavior, addressing the instability and weak supervision issues that arise when scaling latent recurrence with sparse token-level rewards.

## 8. Conclusion

We introduced LoopRPT, a reinforcement pre-training framework for looped language models that addresses the inherent sparsity of token-level feedback. LoopRPT concentrates on learning signals on hard next-token instances and provides step-wise supervision over latent recurrence. Experiments demonstrate that LoopRPT improves next-token reasoning across difficulty levels under both maximum-loop execution and adaptive early exit, while simultaneously reducing the average inference steps. These gains translate to consistent improvements on a diverse set of end-task benchmarks, particularly in math and code, and are accompanied by better-calibrated early-exit behavior. Together, our results suggest that combining looped computation with hard-token-focused RL pre-training is an effective and scalable path toward stronger intermediate reasoning and more efficient inference. Future work includes extending the approach to larger scales and broader data mixtures, and further improving robustness of early-exit calibration under distribution shift.

## References

Austin, J., Odena, A., Nye, M., Bosma, M., Michalewski, H., Dohan, D., Jiang, E., Cai, C., Terry, M., Le, Q., and Sutton, C. Program synthesis with large language mod-

els, 2021. URL <https://arxiv.org/abs/2108.07732>.

Bai, Y., Kadavath, S., Kundu, S., Askell, A., Kernion, J., Jones, A., Chen, A., Goldie, A., Mirhoseini, A., McKinnon, C., Chen, C., Olsson, C., Olah, C., Hernandez, D., Drain, D., Ganguli, D., Li, D., Tran-Johnson, E., Perez, E., Kerr, J., Mueller, J., Ladish, J., Landau, J., Ndousse, K., Lukosuite, K., Lovitt, L., Sellitto, M., Elhage, N., Schiefer, N., Mercado, N., DasSarma, N., Lasenby, R., Larson, R., Ringer, S., Johnston, S., Kravec, S., Showk, S. E., Fort, S., Lanham, T., Telleen-Lawton, T., Conerly, T., Henighan, T., Hume, T., Bowman, S. R., Hatfield-Dodds, Z., Mann, B., Amodei, D., Joseph, N., McCandlish, S., Brown, T., and Kaplan, J. Constitutional ai: Harmlessness from ai feedback, 2022. URL <https://arxiv.org/abs/2212.08073>.

Bajpai, D. J. and Hanawal, M. K. A survey of early exit deep neural networks in nlp, 2025. URL <https://arxiv.org/abs/2501.07670>.

Banino, A., Balaguer, J., and Blundell, C. Pondernet: Learning to ponder, 2021. URL <https://arxiv.org/abs/2107.05407>.

Bulatov, A., Kuratov, Y., and Burtsev, M. Recurrent memory transformer. In Koyejo, S., Mohamed, S., Agarwal, A., Belgrave, D., Cho, K., and Oh, A. (eds.), *Advances in Neural Information Processing Systems*, volume 35, pp. 11079–11091. Curran Associates, Inc., 2022.

Cen, S., Mei, J., Goshvadi, K., Dai, H., Yang, T., Yang, S., Schuurmans, D., Chi, Y., and Dai, B. Value-incentivized preference optimization: A unified approach to online and offline rlhf, 2025. URL <https://arxiv.org/abs/2405.19320>.

Chen, M., Tworek, J., Jun, H., Yuan, Q., de Oliveira Pinto, H. P., Kaplan, J., Edwards, H., Burda, Y., Joseph, N., Brockman, G., Ray, A., Puri, R., Krueger, G., Petrov, M., Khlaaf, H., Sastry, G., Mishkin, P., Chan, B., Gray, S., Ryder, N., Pavlov, M., Power, A., Kaiser, L., Bavarian, M., Winter, C., Tillet, P., Such, F. P., Cummings, D., Plappert, M., Chantzis, F., Barnes, E., Herbert-Voss, A., Guss, W. H., Nichol, A., Paino, A., Tezak, N., Tang, J., Babuschkin, I., Balaji, S., Jain, S., Saunders, W., Hesse, C., Carr, A. N., Leike, J., Achiam, J., Misra, V., Morikawa, E., Radford, A., Knight, M., Brundage, M., Murati, M., Mayer, K., Welinder, P., McGrew, B., Amodei, D., McCandlish, S., Sutskever, I., and Zaremba, W. Evaluating large language models trained on code, 2021. URL <https://arxiv.org/abs/2107.03374>.

Chen, Y., Shang, J., Zhang, Z., Xie, Y., Sheng, J., Liu, T., Wang, S., Sun, Y., Wu, H., and Wang, H. Inner

- thinking transformer: Leveraging dynamic depth scaling to foster adaptive internal thinking, 2025. URL <https://arxiv.org/abs/2502.13842>.
- Christiano, P. F., Leike, J., Brown, T., Martic, M., Legg, S., and Amodei, D. Deep reinforcement learning from human preferences. In Guyon, I., Luxburg, U. V., Bengio, S., Wallach, H., Fergus, R., Vishwanathan, S., and Garnett, R. (eds.), *Advances in Neural Information Processing Systems*, volume 30. Curran Associates, Inc., 2017.
- Clark, P., Cowhey, I., Etzioni, O., Khot, T., Sabharwal, A., Schoenick, C., and Tafjord, O. Think you have solved question answering? try arc, the ai2 reasoning challenge, 2018. URL <https://arxiv.org/abs/1803.05457>.
- Cobbe, K., Kosaraju, V., Bavarian, M., Chen, M., Jun, H., Kaiser, L., Plappert, M., Tworek, J., Hilton, J., Nakano, R., Hesse, C., and Schulman, J. Training verifiers to solve math word problems, 2021. URL <https://arxiv.org/abs/2110.14168>.
- Dai, Z., Yang, Z., Yang, Y., Carbonell, J., Le, Q., and Salakhutdinov, R. Transformer-XL: Attentive language models beyond a fixed-length context. In Korhonen, A., Traum, D., and Màrquez, L. (eds.), *Proceedings of the 57th Annual Meeting of the Association for Computational Linguistics*, pp. 2978–2988, Florence, Italy, July 2019. Association for Computational Linguistics. doi: 10.18653/v1/P19-1285. URL <https://aclanthology.org/P19-1285/>.
- Dehghani, M., Gouws, S., Vinyals, O., Uszkoreit, J., and Łukasz Kaiser. Universal transformers, 2019. URL <https://arxiv.org/abs/1807.03819>.
- Dong, Q., Dong, L., Tang, Y., Ye, T., Sun, Y., Sui, Z., and Wei, F. Reinforcement pre-training. *CoRR*, abs/2506.08007, 2025. doi: 10.48550/ARXIV.2506.08007. URL <https://doi.org/10.48550/arXiv.2506.08007>.
- Ethayarajh, K., Xu, W., Muennighoff, N., Jurafsky, D., and Kiela, D. Kto: Model alignment as prospect theoretic optimization, 2024. URL <https://arxiv.org/abs/2402.01306>.
- Gao, B., Song, F., Yang, Z., Cai, Z., Miao, Y., Dong, Q., Li, L., Ma, C., Chen, L., Xu, R., Tang, Z., Wang, B., Zan, D., Quan, S., Zhang, G., Sha, L., Zhang, Y., Ren, X., Liu, T., and Chang, B. Omni-math: A universal olympiad level mathematic benchmark for large language models, 2024a. URL <https://arxiv.org/abs/2410.07985>.
- Gao, L., Tow, J., Abbasi, B., Biderman, S., Black, S., DiPofi, A., Foster, C., Golding, L., Hsu, J., Le Noac’h, A., Li, H., McDonell, K., Muennighoff, N., Ociepa, C., Phang, J., Reynolds, L., Schoelkopf, H., Skowron, A., Sutawika, L., Tang, E., Thite, A., Wang, B., Wang, K., and Zou, A. The language model evaluation harness, 07 2024b. URL <https://zenodo.org/records/12608602>.
- Grattafiori, A., Dubey, A., Jauhri, A., Pandey, A., Kadian, A., Al-Dahle, A., Letman, A., Mathur, A., Schelten, A., Vaughan, A., et al. The llama 3 herd of models. *arXiv preprint arXiv:2407.21783*, 2024.
- Graves, A. Adaptive computation time for recurrent neural networks. *arXiv preprint arXiv:1603.08983*, 2016.
- Gugger, S., Debut, L., Wolf, T., Schmid, P., Mueller, Z., Mangrulkar, S., Sun, M., and Bossan, B. Accelerate: Training and inference at scale made simple, efficient and adaptable. <https://github.com/huggingface/accelerate>, 2022.
- Guo, D., Yang, D., Zhang, H., Song, J., Wang, P., Zhu, Q., Xu, R., Zhang, R., Ma, S., Bi, X., Zhang, X., Yu, X., Wu, Y., Wu, Z. F., Gou, Z., Shao, Z., Li, Z., Gao, Z., Liu, A., Xue, B., Wang, B., Wu, B., Feng, B., Lu, C., Zhao, C., Deng, C., Ruan, C., Dai, D., Chen, D., Ji, D., Li, E., Lin, F., Dai, F., Luo, F., Hao, G., Chen, G., Li, G., Zhang, H., Xu, H., Ding, H., Gao, H., Qu, H., Li, H., Guo, J., Li, J., Chen, J., Yuan, J., Tu, J., Qiu, J., Li, J., Cai, J. L., Ni, J., Liang, J., Chen, J., Dong, K., Hu, K., You, K., Gao, K., Guan, K., Huang, K., Yu, K., Wang, L., Zhang, L., Zhao, L., Wang, L., Zhang, L., Xu, L., Xia, L., Zhang, M., Zhang, M., Tang, M., Zhou, M., Li, M., Wang, M., Li, M., Tian, N., Huang, P., Zhang, P., Wang, Q., Chen, Q., Du, Q., Ge, R., Zhang, R., Pan, R., Wang, R., Chen, R. J., Jin, R. L., Chen, R., Lu, S., Zhou, S., Chen, S., Ye, S., Wang, S., Yu, S., Zhou, S., Pan, S., Li, S. S., Zhou, S., Wu, S., Yun, T., Pei, T., Sun, T., Wang, T., Zeng, W., Liu, W., Liang, W., Gao, W., Yu, W., Zhang, W., Xiao, W. L., An, W., Liu, X., Wang, X., Chen, X., Nie, X., Cheng, X., Liu, X., Xie, X., Liu, X., Yang, X., Li, X., Su, X., Lin, X., Li, X. Q., Jin, X., Shen, X., Chen, X., Sun, X., Wang, X., Song, X., Zhou, X., Wang, X., Shan, X., Li, Y. K., Wang, Y. Q., Wei, Y. X., Zhang, Y., Xu, Y., Li, Y., Zhao, Y., Sun, Y., Wang, Y., Yu, Y., Zhang, Y., Shi, Y., Xiong, Y., He, Y., Piao, Y., Wang, Y., Tan, Y., Ma, Y., Liu, Y., Guo, Y., Ou, Y., Wang, Y., Gong, Y., Zou, Y., He, Y., Xiong, Y., Luo, Y., You, Y., Liu, Y., Zhou, Y., Zhu, Y. X., Huang, Y., Li, Y., Zheng, Y., Zhu, Y., Ma, Y., Tang, Y., Zha, Y., Yan, Y., Ren, Z. Z., Ren, Z., Sha, Z., Fu, Z., Xu, Z., Xie, Z., Zhang, Z., Hao, Z., Ma, Z., Yan, Z., Wu, Z., Gu, Z., Zhu, Z., Liu, Z., Li, Z., Xie, Z., Song, Z., Pan, Z., Huang, Z., Xu, Z., Zhang, Z., and Zhang, Z. Deepseek-r1 incentivizes reasoning in llms through reinforcement learning. *Nature*, 645(8081):633–638, September 2025. ISSN 1476-4687. doi: 10.1038/s41586-025-09422-z. URL <http://dx.doi.org/10.1038/s41586-025-09422-z>.

- Hatamizadeh, A., Akter, S. N., Prabhunoye, S., Kautz, J., Patwary, M., Shoeybi, M., Catanzaro, B., and Choi, Y. Rlp: Reinforcement as a pretraining objective, 2025. URL <https://arxiv.org/abs/2510.01265>.
- Hendrycks, D., Burns, C., Basart, S., Zou, A., Mazeika, M., Song, D., and Steinhardt, J. Measuring massive multitask language understanding, 2021. URL <https://arxiv.org/abs/2009.03300>.
- Hong, J., Lee, N., and Thorne, J. Orpo: Monolithic preference optimization without reference model, 2024. URL <https://arxiv.org/abs/2403.07691>.
- Jiang, R., Chen, K., Bai, X., He, Z., Li, J., Yang, M., Zhao, T., Nie, L., and Zhang, M. A survey on human preference learning for aligning large language models. *ACM Comput. Surv.*, 58(6), December 2025. ISSN 0360-0300. doi: 10.1145/3773279. URL <https://doi.org/10.1145/3773279>.
- Li, Z., Li, Y., and Zhou, T. Skip a layer or loop it? test-time depth adaptation of pretrained llms, 2025. URL <https://arxiv.org/abs/2507.07996>.
- Liu, J., Xia, C. S., Wang, Y., and Zhang, L. Is your code generated by chatGPT really correct? rigorous evaluation of large language models for code generation. In *Thirty-seventh Conference on Neural Information Processing Systems*, 2023. URL <https://openreview.net/forum?id=lqvx610Cu7>.
- McLeish, S., Li, A., Kirchenbauer, J., Kalra, D. S., Bartoldson, B. R., Kailkhura, B., Schwarzschild, A., Geiping, J., Goldstein, T., and Goldblum, M. Teaching pre-trained language models to think deeper with retrofitted recurrence, 2025. URL <https://arxiv.org/abs/2511.07384>.
- Ouyang, L., Wu, J., Jiang, X., Almeida, D., Wainwright, C., Mishkin, P., Zhang, C., Agarwal, S., Slama, K., Ray, A., Schulman, J., Hilton, J., Kelton, F., Miller, L., Simens, M., Askell, A., Welinder, P., Christiano, P. F., Leike, J., and Lowe, R. Training language models to follow instructions with human feedback. In Koyejo, S., Mohamed, S., Agarwal, A., Belgrave, D., Cho, K., and Oh, A. (eds.), *Advances in Neural Information Processing Systems*, volume 35, pp. 27730–27744. Curran Associates, Inc., 2022.
- Rae, J. W., Potapenko, A., Jayakumar, S. M., and Lillicrap, T. P. Compressive transformers for long-range sequence modelling, 2019. URL <https://arxiv.org/abs/1911.05507>.
- Rafailov, R., Sharma, A., Mitchell, E., Manning, C. D., Ermon, S., and Finn, C. Direct preference optimization: Your language model is secretly a reward model. In Oh, A., Naumann, T., Globerson, A., Saenko, K., Hardt, M., and Levine, S. (eds.), *Advances in Neural Information Processing Systems*, volume 36, pp. 53728–53741. Curran Associates, Inc., 2023.
- Raposo, D., Ritter, S., Richards, B., Lillicrap, T., Humphreys, P. C., and Santoro, A. Mixture-of-depths: Dynamically allocating compute in transformer-based language models, 2024. URL <https://arxiv.org/abs/2404.02258>.
- Sakaguchi, K., Bras, R. L., Bhagavatula, C., and Choi, Y. Winogrande: an adversarial winograd schema challenge at scale. *Commun. ACM*, 64(9):99–106, August 2021. ISSN 0001-0782. doi: 10.1145/3474381. URL <https://doi.org/10.1145/3474381>.
- Schulman, J., Levine, S., Abbeel, P., Jordan, M., and Moritz, P. Trust region policy optimization. In Bach, F. and Blei, D. (eds.), *Proceedings of the 32nd International Conference on Machine Learning*, volume 37 of *Proceedings of Machine Learning Research*, pp. 1889–1897, Lille, France, 07–09 Jul 2015. PMLR. URL <https://proceedings.mlr.press/v37/schulman15.html>.
- Schulman, J., Wolski, F., Dhariwal, P., Radford, A., and Klimov, O. Proximal policy optimization algorithms, 2017. URL <https://arxiv.org/abs/1707.06347>.
- Shao, Z., Wang, P., Zhu, Q., Xu, R., Song, J., Bi, X., Zhang, H., Zhang, M., Li, Y. K., Wu, Y., and Guo, D. Deepseekmath: Pushing the limits of mathematical reasoning in open language models, 2024. URL <https://arxiv.org/abs/2402.03300>.
- Stiennon, N., Ouyang, L., Wu, J., Ziegler, D., Lowe, R., Voss, C., Radford, A., Amodei, D., and Christiano, P. F. Learning to summarize with human feedback. In Larochelle, H., Ranzato, M., Hadsell, R., Balcan, M., and Lin, H. (eds.), *Advances in Neural Information Processing Systems*, volume 33, pp. 3008–3021. Curran Associates, Inc., 2020.
- Suzgun, M., Scales, N., Schärli, N., Gehrmann, S., Tay, Y., Chung, H. W., Chowdhery, A., Le, Q., Chi, E., Zhou, D., and Wei, J. Challenging BIG-bench tasks and whether chain-of-thought can solve them. In Rogers, A., Boyd-Graber, J., and Okazaki, N. (eds.), *Findings of the Association for Computational Linguistics: ACL 2023*, pp. 13003–13051, Toronto, Canada, July 2023. Association for Computational Linguistics. doi: 10.18653/v1/2023.findings-acl.824. URL <https://aclanthology.org/2023.findings-acl.824/>.

- Tan, S., Shen, Y., Chen, Z., Courville, A., and Gan, C. Sparse universal transformer, 2023. URL <https://arxiv.org/abs/2310.07096>.
- Tarvainen, A. and Valpola, H. Mean teachers are better role models: Weight-averaged consistency targets improve semi-supervised deep learning results. *Advances in neural information processing systems*, 30, 2017.
- Team, G., Kamath, A., Ferret, J., Pathak, S., Vieillard, N., Merhej, R., Perrin, S., Matejovicova, T., Ramé, A., Rivière, M., et al. Gemma 3 technical report. *arXiv preprint arXiv:2503.19786*, 2025.
- Team, Q. et al. Qwen2 technical report. *arXiv preprint arXiv:2407.10671*, 2(3), 2024.
- Wang, S., Yu, L., Gao, C., Zheng, C., Liu, S., Lu, R., Dang, K., Chen, X., Yang, J., Zhang, Z., Liu, Y., Yang, A., Zhao, A., Yue, Y., Song, S., Yu, B., Huang, G., and Lin, J. Beyond the 80/20 rule: High-entropy minority tokens drive effective reinforcement learning for llm reasoning, 2025. URL <https://arxiv.org/abs/2506.01939>.
- Wang, Y., Ma, X., Zhang, G., Ni, Y., Chandra, A., Guo, S., Ren, W., Arulraj, A., He, X., Jiang, Z., Li, T., Ku, M., Wang, K., Zhuang, A., Fan, R., Yue, X., and Chen, W. Mmlu-pro: A more robust and challenging multi-task language understanding benchmark. In Globerson, A., Mackey, L., Belgrave, D., Fan, A., Paquet, U., Tomczak, J., and Zhang, C. (eds.), *Advances in Neural Information Processing Systems*, volume 37, pp. 95266–95290. Curran Associates, Inc., 2024. doi: 10.52202/079017-3018.
- Wei, J., Wang, X., Schuurmans, D., Bosma, M., Xia, F., Chi, E., Le, Q. V., Zhou, D., et al. Chain-of-thought prompting elicits reasoning in large language models. *Advances in neural information processing systems*, 35:24824–24837, 2022.
- Wen, X., Liu, Z., Zheng, S., Ye, S., Wu, Z., Wang, Y., Xu, Z., Liang, X., Li, J., Miao, Z., Bian, J., and Yang, M. Reinforcement learning with verifiable rewards implicitly incentivizes correct reasoning in base llms, 2025. URL <https://arxiv.org/abs/2506.14245>.
- Wolf, T., Debut, L., Sanh, V., Chaumond, J., Delangue, C., Moi, A., Cistac, P., Rault, T., Louf, R., Funtowicz, M., Davison, J., Shleifer, S., von Platen, P., Ma, C., Jernite, Y., Plu, J., Xu, C., Scao, T. L., Gugger, S., Drame, M., Lhoest, Q., and Rush, A. M. Transformers: State-of-the-art natural language processing. In *Proceedings of the 2020 Conference on Empirical Methods in Natural Language Processing: System Demonstrations*, pp. 38–45, Online, October 2020. Association for Computational Linguistics. URL <https://www.aclweb.org/anthology/2020.emnlp-demos.6>.
- Wu, B., Chen, M., Luo, X., Yan, S., Yu, Q., Xia, F., Zhang, T., Zhan, H., Zhong, Z., Zhou, X., Qiao, S., and Bin, X. Parallel loop transformer for efficient test-time computation scaling, 2025. URL <https://arxiv.org/abs/2510.24824>.
- Xiao, W., Wang, Z., Gan, L., Zhao, S., Li, Z., Lei, R., He, W., Tuan, L. A., Chen, L., Jiang, H., Zhao, Z., and Wu, F. A comprehensive survey of direct preference optimization: Datasets, theories, variants, and applications, 2025. URL <https://arxiv.org/abs/2410.15595>.
- Xin, J., Tang, R., Lee, J., Yu, Y., and Lin, J. Deebert: Dynamic early exiting for accelerating bert inference, 2020. URL <https://arxiv.org/abs/2004.12993>.
- Xu, C. and McAuley, J. A survey on dynamic neural networks for natural language processing. In Vlachos, A. and Augenstein, I. (eds.), *Findings of the Association for Computational Linguistics: EACL 2023*, pp. 2370–2381, Dubrovnik, Croatia, May 2023. Association for Computational Linguistics. doi: 10.18653/v1/2023.findings-eacl.180. URL <https://aclanthology.org/2023.findings-eacl.180/>.
- Yang, A., Li, A., Yang, B., Zhang, B., Hui, B., Zheng, B., Yu, B., Gao, C., Huang, C., Lv, C., et al. Qwen3 technical report. *arXiv preprint arXiv:2505.09388*, 2025.
- Zellers, R., Holtzman, A., Bisk, Y., Farhadi, A., and Choi, Y. Hellaswag: Can a machine really finish your sentence?, 2019. URL <https://arxiv.org/abs/1905.07830>.
- Zeng, B., Li, H., Song, S., Wang, Y., He, Z., Wang, X., and Lin, Z. Ponderlm-2: Pretraining llm with latent thoughts in continuous space, 2025. URL <https://arxiv.org/abs/2509.23184>.
- Zhou, W., Xu, C., Ge, T., McAuley, J., Xu, K., and Wei, F. Bert loses patience: Fast and robust inference with early exit. In Larochelle, H., Ranzato, M., Hadsell, R., Balcan, M., and Lin, H. (eds.), *Advances in Neural Information Processing Systems*, volume 33, pp. 18330–18341. Curran Associates, Inc., 2020.
- Zhu, R.-J., Wang, Z., Hua, K., Zhang, T., Li, Z., Que, H., Wei, B., Wen, Z., Yin, F., Xing, H., et al. Scaling latent reasoning via looped language models. *arXiv preprint arXiv:2510.25741*, 2025.

## A. Additional Theory

**Setup and notation.** For a fixed next-token position  $t$  in a sequence, LoopRPT defines: (i) a teacher (EMA) model  $\bar{\theta}$  and a student model  $\theta$ ; (ii) a teacher exit distribution  $\pi_{\bar{\theta}}(k)$  and student exit distribution  $\pi_{\theta}(k)$  over latent steps  $k \in \{1, \dots, K\}$  (Eq. (2–3)); (iii) a teacher reference step  $t_{\text{ref}} = \min\{k : \sum_{j \leq k} \pi_{\bar{\theta}}(j) \geq \tau\}$ ; (iv) a per-token dynamic baseline  $b_{\text{ref}} = \ell_{\bar{\theta}}^{(t_{\text{ref}})}$  (Eq. (5)); (v) a step-wise reward  $R(k) = \Delta_{\text{acc}}(k) - C(k)$  (Eq. (9)) where  $\Delta_{\text{acc}}(k) = \ell_{\theta}^{(k)} - b_{\text{ref}}$  (Eq. (6)) and  $C(k) = \lambda_t(k - t_{\text{ref}})$  (Eq. (7)), with  $\lambda_t$  derived from teacher uncertainty (Eq. (8)). We use  $\Pi_{\theta}(k) := \sum_{j \leq k} \pi_{\theta}(j)$  to denote the CDF.

### A.1. Why High-Entropy Token Selection Focuses Training Signal

**Teacher entropy and selection.** LoopRPT computes teacher entropy (Eq. (4)):

$$H_t := - \sum_{v \in V} \bar{p}_{\bar{\theta}}(v | x_{<t}) \log \bar{p}_{\bar{\theta}}(v | x_{<t}), \quad (17)$$

and selects the top- $\rho$  fraction of positions within each example as hard tokens (Sec. 3.2).

**A principled proxy: expected gradient energy.** We justify entropy selection by relating teacher uncertainty to the *expected squared norm* of the cross-entropy gradient, a standard proxy for how informative a sample is for learning.

**Assumption A.1** (Teacher distribution as a proxy for label uncertainty). Conditioned on context  $x_{<t}$ , the ground-truth next token  $y$  is drawn from the teacher distribution  $\bar{p}(v) := \bar{p}_{\bar{\theta}}(v | x_{<t})$ .

**Cross-entropy gradient.** Let the student predictive distribution be  $q(v) := p_{\theta}(v | x_{<t})$ . For a single sampled label  $y$ , the negative log-likelihood is  $\mathcal{L}(q; y) = -\log q(y)$ . Differentiating w.r.t. the student logits  $z$  (where  $q = \text{Softmax}(z)$ ) yields the well-known form:

$$\nabla_z \mathcal{L}(q; y) = q - e_y, \quad (18)$$

where  $e_y$  is the one-hot vector.

**Lemma A.2** (Expected gradient energy depends on collision probability). *Under Assumption A.1, the expected squared  $\ell_2$ -norm of the logit-gradient is*

$$\mathbb{E}_{y \sim \bar{p}} [\|\nabla_z \mathcal{L}(q; y)\|_2^2] = \|q\|_2^2 + 1 - 2\langle q, \bar{p} \rangle. \quad (19)$$

*In particular, when the student matches the teacher locally ( $q = \bar{p}$ ),*

$$\mathbb{E}_{y \sim \bar{p}} [\|\nabla_z \mathcal{L}(\bar{p}; y)\|_2^2] = 1 - \|\bar{p}\|_2^2. \quad (20)$$

*Proof.* Using (18),

$$\|\nabla_z \mathcal{L}(q; y)\|_2^2 = \|q - e_y\|_2^2 = \|q\|_2^2 + \|e_y\|_2^2 - 2\langle q, e_y \rangle = \|q\|_2^2 + 1 - 2q(y).$$

Taking expectation over  $y \sim \bar{p}$  gives  $\mathbb{E}[q(y)] = \sum_v \bar{p}(v)q(v) = \langle q, \bar{p} \rangle$ , which yields (19). Setting  $q = \bar{p}$  gives (20).  $\square$

**Relating collision probability to entropy.** Define the collision probability  $c(\bar{p}) := \|\bar{p}\|_2^2 = \sum_v \bar{p}(v)^2$ . The (order-2) Rényi entropy is  $H_2(\bar{p}) := -\log c(\bar{p})$ , and it is standard that Shannon entropy upper-bounds Rényi-2 entropy:

$$H_t \geq H_2(\bar{p}) = -\log \|\bar{p}\|_2^2. \quad (21)$$

Equivalently,

$$\|\bar{p}\|_2^2 \leq e^{-H_t}. \quad (22)$$

**Proposition A.3** (High entropy implies large expected gradient energy). *Under Assumption A.1 and local student-teacher agreement ( $q = \bar{p}$ ), the expected gradient energy satisfies*

$$\mathbb{E}_{y \sim \bar{p}} [\|\nabla_z \mathcal{L}(\bar{p}; y)\|_2^2] = 1 - \|\bar{p}\|_2^2 \geq 1 - e^{-H_t}. \quad (23)$$

*Thus, larger teacher entropy  $H_t$  yields a (monotone) larger lower bound on gradient energy.*

*Proof.* Combine (20) with (22):  $1 - \|\bar{p}\|_2^2 \geq 1 - e^{-H_t}$ . Monotonicity follows since  $1 - e^{-H_t}$  increases in  $H_t$ .  $\square$

**Connection to LoopRPT.** LoopRPT selects top- $\rho$  high-entropy tokens using (17). Proposition A.3 shows that, under a standard uncertainty-as-label-proxy assumption, higher teacher entropy provably implies larger expected cross-entropy gradient energy (and hence more informative updates) near local student-teacher agreement. This provides a principled explanation for why focusing losses (Sec. 3.3–3.4) on high-entropy positions improves sample-efficiency and amplifies useful training signals.

## A.2. Noisy Latent Rollouts Optimize a Smoothed On-Policy Objective

**Noisy latent rollouts.** LoopRPT injects Gaussian noise into the recurrent latent states (Eq. (11)):

$$h^{(k)} \leftarrow h^{(k)} + \epsilon^{(k)}, \quad \epsilon^{(k)} \sim \mathcal{N}(0, \sigma^2 I). \quad (24)$$

Let  $\epsilon := \{\epsilon^{(k)}\}_{k=1}^K$  denote the full noise trajectory, and write the resulting (noisy) exit distribution as  $\pi_{\theta, \epsilon}(k)$ . Under *reward regain*, the per-step student log-probability is recomputed on the same noisy trajectory, denoted  $\ell_{\theta, \epsilon}^{(k)}$ , and the step-wise reward is

$$R_\epsilon(k) := \underbrace{(\ell_{\theta, \epsilon}^{(k)} - b_{\text{ref}})}_{\Delta_{\text{acc}, \epsilon}(k)} - \underbrace{\lambda_t(k - t_{\text{ref}})}_{C(k)}. \quad (25)$$

This mirrors Eq. (6–9) with  $\ell_\theta^{(k)}$  replaced by  $\ell_{\theta, \epsilon}^{(k)}$ .

**Definition A.4** (Smoothed on-policy objective induced by latent noise). Define

$$J_\sigma(\theta) := \mathbb{E}_{\epsilon \sim \mathcal{N}(0, \sigma^2 I)} \left[ \sum_{k=1}^K \pi_{\theta, \epsilon}(k) R_\epsilon(k) \right] = \mathbb{E}_\epsilon \mathbb{E}_{k \sim \pi_{\theta, \epsilon}} [R_\epsilon(k)]. \quad (26)$$

**Key technical point.** In the policy-gradient term of LoopRPT (Eq. (13)),  $R_\epsilon(k)$  is used as a scalar reward signal. Accordingly, we analyze the score-function gradient, i.e., we do not backpropagate through the internal computation of  $R_\epsilon(k)$ .

**Proposition A.5** (Exact score-function gradient of  $J_\sigma$ ). *Under the above convention (treating  $R_\epsilon(k)$  as a reward signal), the gradient of  $J_\sigma$  is*

$$\nabla_\theta J_\sigma(\theta) = \mathbb{E}_\epsilon \mathbb{E}_{k \sim \pi_{\theta, \epsilon}} [R_\epsilon(k) \nabla_\theta \log \pi_{\theta, \epsilon}(k)]. \quad (27)$$

Consequently, Monte Carlo estimation using  $G$  i.i.d. noisy rollouts yields an unbiased estimator of the right-hand side of (27).

*Proof.* By Definition A.4,

$$J_\sigma(\theta) = \mathbb{E}_\epsilon \sum_{k=1}^K \pi_{\theta, \epsilon}(k) R_\epsilon(k).$$

Treat  $R_\epsilon(k)$  as constant w.r.t.  $\theta$  in this gradient (score-function convention):

$$\nabla_\theta J_\sigma(\theta) = \mathbb{E}_\epsilon \sum_{k=1}^K R_\epsilon(k) \nabla_\theta \pi_{\theta, \epsilon}(k).$$

Using  $\nabla_\theta \pi = \pi \nabla_\theta \log \pi$  gives

$$\nabla_\theta J_\sigma(\theta) = \mathbb{E}_\epsilon \sum_{k=1}^K \pi_{\theta, \epsilon}(k) R_\epsilon(k) \nabla_\theta \log \pi_{\theta, \epsilon}(k) = \mathbb{E}_\epsilon \mathbb{E}_{k \sim \pi_{\theta, \epsilon}} [R_\epsilon(k) \nabla_\theta \log \pi_{\theta, \epsilon}(k)],$$

which is (27). Unbiasedness of the Monte Carlo estimate follows from linearity of expectation.  $\square$

**Proposition A.6** (Gaussian smoothing yields robustness bounds). *Assume for a fixed  $\theta$  that the per-noise rollout objective  $F(\epsilon) := \mathbb{E}_{k \sim \pi_{\theta, \epsilon}} [R_\epsilon(k)]$  is  $L$ -Lipschitz in  $\epsilon$ :  $|F(\epsilon) - F(\epsilon')| \leq L \|\epsilon - \epsilon'\|$ . Then*

$$|J_\sigma(\theta) - F(0)| = |\mathbb{E}_\epsilon [F(\epsilon)] - F(0)| \leq L \mathbb{E} \|\epsilon\|. \quad (28)$$

Moreover, for  $\epsilon \sim \mathcal{N}(0, \sigma^2 I_d)$ , we have the explicit bound  $\mathbb{E} \|\epsilon\| \leq \sigma \sqrt{d}$ , hence  $|J_\sigma(\theta) - F(0)| \leq L \sigma \sqrt{d}$ .

*Proof.* By Jensen and Lipschitzness,  $|\mathbb{E}F(\epsilon) - F(0)| \leq \mathbb{E}|F(\epsilon) - F(0)| \leq L\mathbb{E}\|\epsilon\|$ , which is (28). For a Gaussian vector in  $\mathbb{R}^d$ ,  $\mathbb{E}\|\epsilon\| \leq \sqrt{\mathbb{E}\|\epsilon\|^2} = \sqrt{\mathbb{E}\sum_{i=1}^d \epsilon_i^2} = \sigma\sqrt{d}$ .  $\square$

**Connection to LoopRPT.** LoopRPT’s noisy latent rollouts (Eq. (13)) induce the smoothed on-policy objective  $J_\sigma$  in (26). Proposition A.5 formalizes that, under the standard score-function convention used in the policy-gradient term, the rollout gradient estimates the exact gradient of this smoothed objective. Proposition A.6 further shows that latent Gaussian noise replaces a potentially brittle deterministic rollout objective  $F(0)$  by its Gaussian average, which is robust to local perturbations with a deviation controlled by  $\sigma$ ; this provides a theoretical justification for improved stability when learning exit behaviors from latent-space variability.

### A.3. EMA Teacher as a Provably Slowly Moving Reference

**EMA update.** LoopRPT maintains an EMA teacher updated after each student step:

$$\bar{\theta}_n = \phi\bar{\theta}_{n-1} + (1 - \phi)\theta_n, \quad \phi \in [0, 1). \quad (29)$$

**Lemma A.7** (Closed form and lag decomposition). *For any  $n \geq 1$ ,*

$$\bar{\theta}_n = \phi^n\bar{\theta}_0 + (1 - \phi)\sum_{i=1}^n \phi^{n-i}\theta_i. \quad (30)$$

Moreover, defining parameter increments  $\Delta_i := \theta_i - \theta_{i-1}$ , we have the exact identity

$$\theta_n - \bar{\theta}_n = \phi^n(\theta_0 - \bar{\theta}_0) + \sum_{i=1}^n \phi^{n-i}\Delta_i. \quad (31)$$

*Proof.* Unrolling (29) yields (30) by induction. For (31), subtract (30) from  $\theta_n$ :

$$\theta_n - \bar{\theta}_n = \theta_n - \phi^n\bar{\theta}_0 - (1 - \phi)\sum_{i=1}^n \phi^{n-i}\theta_i.$$

Rewrite  $\theta_n$  as  $\phi^n\theta_0 + \sum_{i=1}^n \phi^{n-i}(\theta_i - \phi\theta_{i-1})$  and collect terms to obtain the stated decomposition in  $\Delta_i$  (details follow from telescoping).  $\square$

**Interpretation.** Eq. (31) shows the teacher *lags* behind the student by a geometrically weighted sum of recent student updates  $\{\Delta_i\}$ ; hence  $\bar{\theta}$  is a low-pass filtered version of  $\theta$ .

**Assumption A.8** (Lipschitz mapping from parameters to exit CDF). For any  $k \in \{1, \dots, K\}$  and any context  $x_{<t}$ , there exists  $L_\Pi > 0$  such that

$$|\Pi_\theta(k) - \Pi_{\theta'}(k)| \leq L_\Pi\|\theta - \theta'\|. \quad (32)$$

**Proposition A.9** (Teacher reference step is stable under small drift). *Fix  $(x_{<t})$  and suppose for some  $k^*$  there is a margin  $m > 0$  such that*

$$\Pi_{\bar{\theta}_{n-1}}(k^* - 1) \leq \tau - m \quad \text{and} \quad \Pi_{\bar{\theta}_{n-1}}(k^*) \geq \tau + m. \quad (33)$$

*If  $\|\bar{\theta}_n - \bar{\theta}_{n-1}\| \leq \frac{m}{L_\Pi}$ , then the teacher reference step computed from  $\bar{\theta}_n$  remains unchanged:  $t_{\text{ref}}(\bar{\theta}_n) = k^*$ .*

*Proof.* By Assumption A.8, for any  $k$ ,  $|\Pi_{\bar{\theta}_n}(k) - \Pi_{\bar{\theta}_{n-1}}(k)| \leq L_\Pi\|\bar{\theta}_n - \bar{\theta}_{n-1}\| \leq m$ . Hence

$$\Pi_{\bar{\theta}_n}(k^* - 1) \leq \Pi_{\bar{\theta}_{n-1}}(k^* - 1) + m \leq (\tau - m) + m = \tau,$$

and

$$\Pi_{\bar{\theta}_n}(k^*) \geq \Pi_{\bar{\theta}_{n-1}}(k^*) - m \geq (\tau + m) - m = \tau.$$

Therefore the minimum  $k$  such that  $\Pi_{\bar{\theta}_n}(k) \geq \tau$  is still  $k^*$ .  $\square$

**Proposition A.10** (EMA yields  $O(1 - \phi)$  consecutive-teacher drift). *For the EMA update (29),*

$$\|\bar{\theta}_n - \bar{\theta}_{n-1}\| = (1 - \phi)\|\theta_n - \bar{\theta}_{n-1}\|. \quad (34)$$

*In particular, when  $\theta_n$  and  $\bar{\theta}_{n-1}$  are close (typical in late training), the teacher drift is suppressed by the factor  $(1 - \phi)$ .*

*Proof.* Subtract  $\bar{\theta}_{n-1}$  from (29):  $\bar{\theta}_n - \bar{\theta}_{n-1} = (1 - \phi)(\theta_n - \bar{\theta}_{n-1})$ . Taking norms yields (34).  $\square$

**Connection to LoopRPT.** LoopRPT computes  $t_{\text{ref}}$  (Sec. 3.3) and  $b_{\text{ref}} = \ell_{\bar{\theta}}^{(t_{\text{ref}})}$  (Eq. (5)) from the teacher. Proposition A.10 shows that EMA makes the teacher a slowly moving reference, and Proposition A.9 further implies that whenever the teacher CDF crosses the exit threshold with a nontrivial margin, the discrete reference step  $t_{\text{ref}}$  is invariant to small parameter drift. Together, these results formalize why EMA reduces “target chasing” when jointly optimizing the exit policy and intermediate representations.

## B. Full Training Algorithm

Alg. 1–2 provides a description of our training iteration. The algorithm uses two phases: (i) a no-gradient phase that constructs a dense step-wise reward table for each selected token, and (ii) a gradient phase that jointly optimizes the exit policy via noisy latent rollouts and the backbone via step-weighted next-token learning.

## C. Online Hard-token Selection Details

We perform entropy-based filtering on-the-fly and apply reinforcement-style losses only to the top- $\rho$  high-entropy tokens, following the high-entropy minority token selection strategy in Wang et al. (2025). Concretely, we compute token entropies using the teacher’s *final* latent step, which reflects the model’s most refined uncertainty estimate for next-token prediction.

Let  $\mathbf{h}_{\bar{\theta}}^{(K)}$  be the teacher hidden state at the last loop step. We compute logits and shift them for next-token alignment:

$$\mathbf{z}_{\bar{\theta}}^{(K)} = \text{LMHead}(\mathbf{h}_{\bar{\theta}}^{(K)}) \in \mathbb{R}^{B \times S \times |\mathcal{V}|}, \quad \tilde{\mathbf{z}} = \mathbf{z}_{\bar{\theta}}^{(K)}(:, 1 : -1, :) \in \mathbb{R}^{B \times (S-1) \times |\mathcal{V}|}. \quad (35)$$

The per-token entropy is then

$$H_{i,t} = - \sum_{v \in \mathcal{V}} p_{i,t}(v) \log p_{i,t}(v), \quad p_{i,t} = \text{Softmax}(\tilde{\mathbf{z}}_{i,t,:}). \quad (36)$$

We restrict selection to valid training positions using the shifted loss mask  $\mathbf{m} \in \{0, 1\}^{B \times (S-1)}$  (response tokens). For each example  $i$ , we compute a *row-wise* quantile threshold over valid positions,

$$q_i = \text{Quantile}(\{H_{i,t} : \mathbf{m}_{i,t} = 1\}, 1 - \rho), \quad (37)$$

and define the entropy mask

$$\mathbf{m}_{\text{RPT},i,t} = \mathbb{I}[H_{i,t} > q_i]. \quad (38)$$

Finally, we update the effective training mask by elementwise multiplication,

$$\mathbf{m} \leftarrow \mathbf{m} \odot \mathbf{m}_{\text{RPT}}, \quad (39)$$

so all subsequent losses are computed only on the selected high-entropy positions.

## D. K3-style KL surrogate

We regularize the student against the EMA teacher using the same stable surrogate. For a given step  $k$ , let  $\ell_{\theta}^{(k)}$  and  $\ell_{\bar{\theta}}^{(k)}$  be the student/teacher log-probabilities of the gold next token. Define the log-ratio

$$\Delta^{(k)} = \ell_{\bar{\theta}}^{(k)} - \ell_{\theta}^{(k)}. \quad (40)$$

Optionally, we clamp  $\Delta^{(k)}$  to a bounded range. We then compute

$$u^{(k)} = \exp(\Delta^{(k)}), \quad K3^{(k)} = u^{(k)} - \Delta^{(k)} - 1, \quad (41)$$

and clamp  $K3^{(k)}$  to stabilize optimization. Finally, we weight the per-step KL surrogate on the noisy rollout forward pass using the rollout masks  $\mathbf{m}^G$ , and average over masked tokens:

$$\mathcal{L}_{KL} = \frac{\sum(\sum_k K3^{(k)}) \odot \mathbf{m}^G}{\sum \mathbf{m}^G + \epsilon}. \quad (42)$$

## E. Details of Datasets

**MMLU (Hendrycks et al., 2021)** MMLU<sup>9</sup> is a multi-domain multiple-choice benchmark covering 57 subjects, designed to test broad factual knowledge and general reasoning.

**MMLU-Pro (Wang et al., 2024)** MMLU-Pro<sup>10</sup> is an updated variant of MMLU with more challenging questions and stricter evaluation protocols to reduce ambiguity and contamination effects.

**BBH (Suzgun et al., 2023)** BIG-Bench Hard (BBH)<sup>11</sup> is a curated subset of BIG-Bench tasks emphasizing compositional and multi-step reasoning (e.g., logical deduction, symbolic manipulation).

**ARC-Challenge (ARC-C) (Clark et al., 2018)** ARC-C<sup>12</sup> is a grade-school science multiple-choice benchmark focusing on difficult questions that require reasoning beyond surface pattern matching.

**HellaSwag (Zellers et al., 2019)** HellaSwag<sup>13</sup> evaluates commonsense narrative completion by selecting the most plausible continuation among candidates.

**Winogrande (Sakaguchi et al., 2021)** Winogrande<sup>14</sup> is a large-scale pronoun resolution benchmark that tests commonsense reasoning and bias-sensitive coreference decisions.

**GSM8K (Cobbe et al., 2021)** GSM8K<sup>15</sup> is a grade-school math word-problem benchmark that requires multi-step arithmetic reasoning.

**HumanEval (Chen et al., 2021)** HumanEval<sup>16</sup> is a code-generation benchmark consisting of programming problems with unit-test based evaluation.

**HumanEval+ (Liu et al., 2023)** HumanEval+<sup>17</sup> extends HumanEval with additional and harder tests to reduce overfitting to the original unit tests and better measure functional correctness.

**MBPP (Austin et al., 2021)** MBPP (Mostly Basic Programming Problems)<sup>18</sup> is a Python programming benchmark covering short, diverse coding tasks with reference tests.

**MBPP+ (Liu et al., 2023)** MBPP+<sup>19</sup> strengthens MBPP by adding more comprehensive test suites, improving robustness of functional evaluation.

<sup>9</sup><https://huggingface.co/datasets/cais/mmlu>

<sup>10</sup><https://huggingface.co/datasets/TIGER-Lab/MMLU-Pro>

<sup>11</sup><https://github.com/suzgunmirac/BIG-Bench-Hard>

<sup>12</sup>[https://huggingface.co/datasets/allenai/ai2\\_arc](https://huggingface.co/datasets/allenai/ai2_arc)

<sup>13</sup><https://huggingface.co/datasets/Rowan/hellaswag>

<sup>14</sup><https://huggingface.co/datasets/allenai/winogrande>

<sup>15</sup><https://huggingface.co/datasets/openai/gsm8k>

<sup>16</sup>[https://huggingface.co/datasets/openai/openai\\_humaneval](https://huggingface.co/datasets/openai/openai_humaneval)

<sup>17</sup><https://huggingface.co/datasets/evalplus/humanevalplus>

<sup>18</sup><https://huggingface.co/datasets/google-research-datasets/mbpp>

<sup>19</sup><https://huggingface.co/datasets/evalplus/mbppplus>

**Omni-Math (Gao et al., 2024a)** OMNI-MATH<sup>20</sup> is a benchmark for evaluating mathematical reasoning in large language models, composed of problems drawn from international mathematics competitions. The dataset emphasizes multi-step reasoning and symbolic manipulation.

## F. Additional Experimental Details

### F.1. Training Hyperparameters and Infrastructure

We implement our training pipeline using Hugging Face (Wolf et al., 2020) and Accelerate (Gugger et al., 2022), and speed up training with Distributed Data Parallel, mixed precision, and gradient checkpointing. We train for 3 epochs with a maximum sequence length of 4096 and use the AdamW optimizer. We apply a cosine decay learning rate schedule with a warmup phase to stabilize training. For each training example, we independently sample 8 times from an isotropic Gaussian distribution,  $\epsilon \sim \mathcal{N}(0, \sigma^2 I)$  with  $\sigma = 0.1$  (i.e., variance 0.01), yielding 8 distinct OURO latent trajectories. All hyperparameters are summarized in Table 5. All experiments are conducted on 8 NVIDIA A100 GPUs with 80GB memory. Each training run takes approximately 2 hours for Ouro-1.4B and around 4 hours for Ouro-2.6B.

Table 5. Hyperparameters used for LoopRPT Training.

Params	Values
Gradient clip norm	1.0
Teacher update momentum $\phi$	0.995
Batch size	8
Epoch number	3
Rollout number	8
Learning rate	$5 \times 10^{-6}$
AdamW	(0.9, 0.999)
Weight decay	0.01
Warmup radio	0.03
Max sequence length	4096
Top-Entropy radio $\rho$	0.2
Time penalty base coefficient $\lambda_{\text{base}}$	0.02
Time penalty scale coefficient $\lambda_{\text{scale}}$	0.5
Policy-gradient loss coefficient $\alpha$	1.0
Backbone loss coefficient $\beta$	1.0
KL loss coefficient $\delta$	0.0001
Entropy loss coefficient $\gamma$	0.01

### F.2. Detailed Evaluation Settings

We conducted a comprehensive evaluation of the LoopRPT trained Ouro model, focusing on its performance improvements over the original model in general knowledge, reasoning, mathematics, science, coding, and multilingual capabilities. We also compared it with open-source base models of similar scale to Ouro, including the Qwen2.5 (Team et al., 2024), Qwen3 (Yang et al., 2025), Gemma3 (Team et al., 2025), LLaMA3.1 (Grattafiori et al., 2024), and LLaMA3.2 (Grattafiori et al., 2024) series. Following Ouro (Zhu et al., 2025), all evaluations were conducted using lm-eval-harness (Gao et al., 2024b) and evalplus (Liu et al., 2023). Detailed evaluation settings and metrics are provided in Table 6.

## G. Training Dynamics Visualization

Figure 8 and 9 visualizes the training dynamics of LoopRPT on Ouro. Subfigure (a) tracks validation next-token accuracy under maximum-loop inference (Peak) and adaptive early exit (Adap.), together with the average exit steps. Subfigure (b) shows the evolution of the student’s exit behavior relative to the EMA teacher reference: we report rolling-mean

<sup>20</sup><https://huggingface.co/datasets/KbsdJames/Omni-MATH>

Table 6. Evaluation settings and frameworks of benchmarks.

Benchmark	Settings	Framework
<i>General</i>		
MMLU	logprobs, 5-shot	lm-eval-harness
MMLU-Pro	strict match, 5-shot CoT	lm-eval-harness
BBH	strict match, 3-shot CoT	lm-eval-harness
ARC-C	logprobs, 25-shot	lm-eval-harness
HellaSwag	logprobs, 10-shot	lm-eval-harness
Winogrande	logprobs, 5-shot	lm-eval-harness
<i>Math</i>		
GSM8k	strict match, 3-shot CoT	lm-eval-harness
<i>Code</i>		
HumanEval	pass@1	evalplus
HumanEval+	pass@1	evalplus
MBPP	pass@1	evalplus
MBPP+	pass@1	evalplus

reasoning steps and the student’s within-window variability. Overall, the curves indicate that LoopRPT improves validation performance while progressively reducing the required reasoning steps, consistent with better early-exit calibration.

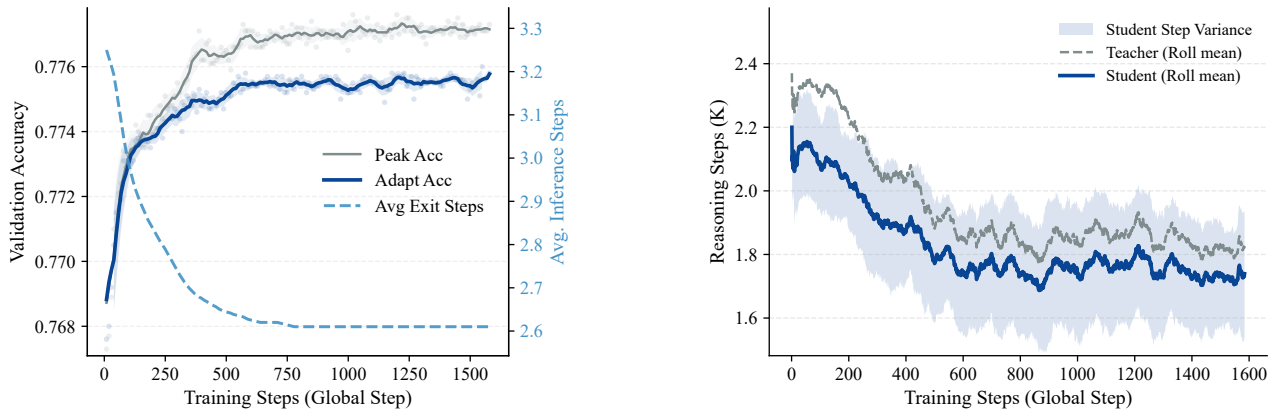
## H. Case Studies

To further investigate the underlying reasoning mechanisms of LoopRPT compared to the base Ouro model, we conduct a detailed qualitative analysis across three distinct domains: general reasoning, mathematical problem-solving, and code generation. As illustrated in Fig. 10, Fig. 11, and Fig. 12, these cases highlight the robust error-correction and multi-step dependency tracking capabilities of our model.

**General reasoning & factual consistency.** In complex scenarios requiring interdisciplinary knowledge (e.g., thermodynamics and biology), the base model frequently exhibits *factual hallucinations* or *logical fragility*. For instance, in Case 2 (Biology), the base model incorrectly categorizes birds as ectotherms despite mentioning their endothermic nature later in the trace. In contrast, LoopRPT maintains high factual consistency throughout the reasoning chain. In Case 3 (Discrete Logic), LoopRPT successfully identifies implicit logical equivalences between different Boolean expressions, whereas the base model fails to recognize the semantic overlap, leading to incomplete conclusions.

**Mathematical logic & constraint satisfaction.** The mathematical cases on GSM8K reveal that the base model is prone to *variable mapping errors* and *set-neglect*. In Case 1 (Scheduling), the base model confuses the count of inpatients with appointments, whereas LoopRPT meticulously tracks separate constraints. Notably, in Case 2 (Finance) and Case 3 (Fractional Calculation), the base model fails to maintain the global state of sets (e.g., neglecting the combined total of two agents). LoopRPT demonstrates a superior ability to iterate through multi-step arithmetic constraints, likely benefiting from the implicit loops that reinforce state tracking.

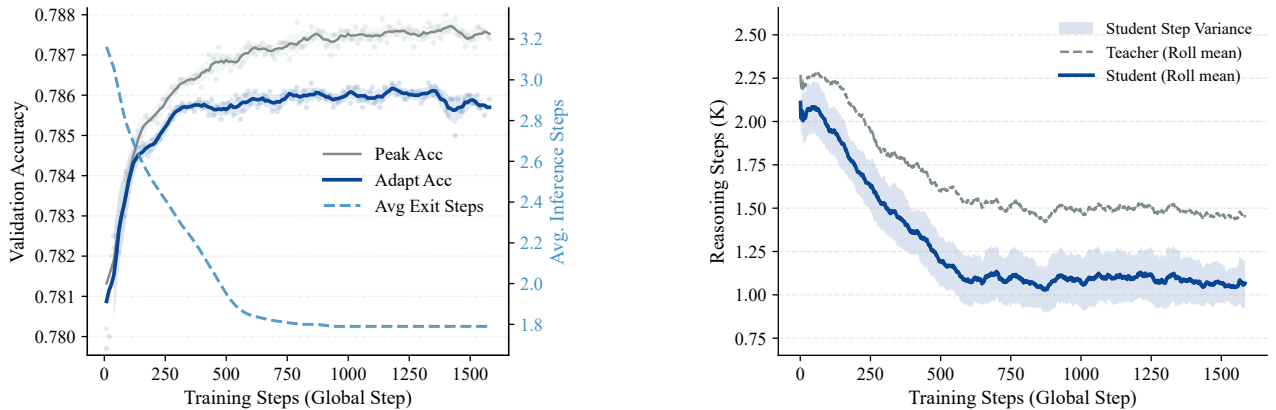
**Algorithmic invariants in coding.** On coding benchmarks (MBPP and HumanEval), the divergence is primarily seen in *boundary condition handling* and *algorithmic interpretation*. The base model often produces “off-by-one” errors (Case 2) or fails to identify cyclic invariants in array operations (Case 3). LoopRPT consistently generates code that adheres to task-specific constraints and rigorous logic. This suggests that the latent reasoning loops in LoopRPT act as a form of implicit verification, allowing the model to simulate execution states more effectively than standard autoregressive generation.



(a) **Validation accuracy-compute trade-off.** We report validation next-token accuracy under maximum-loop inference (Peak Acc) and adaptive early exit (Adapt Acc), together with the average exit steps (right y-axis). Faint dots indicate raw evaluation points and shaded bands reflect locally smoothed variability.

(b) **Evolution of early-exit behavior during training.** We plot the rolling-mean reasoning steps of the student (solid) and the EMA teacher reference (dashed); the shaded region shows the student’s within-window variability. The student progressively aligns with the reference while converging to fewer steps, indicating improved early-exit calibration.

Figure 8. Training dynamics of LoopRPT on Ouro-1.4B.



(a) **Validation accuracy-compute trade-off.** We report validation next-token accuracy under maximum-loop inference (Peak Acc) and adaptive early exit (Adapt Acc), together with the average exit steps (right y-axis). Faint dots indicate raw evaluation points and shaded bands reflect locally smoothed variability.

(b) **Evolution of early-exit behavior during training.** We plot the rolling-mean reasoning steps of the student (solid) and the EMA teacher reference (dashed); the shaded region shows the student’s within-window variability. The student progressively aligns with the reference while converging to fewer steps, indicating improved early-exit calibration.

Figure 9. Training dynamics of LoopRPT on Ouro-2.6B.

**Case Analysis on General Tasks (MMLU-Pro)**

**Case 1: Engineering (Thermodynamics)**

**Question:** Three kilograms of air are at an initial state of 100kPa, 300°K. The air is then compressed polytropically with  $n = 2.56$ , to a final pressure of 500kPa. Assuming constant specific heats, calculate the change in entropy using the three ideal gas equations.  
**Options:** (A) 2.50 kJ/°K (B) 1.25 kJ/°K (C) 2.00 kJ/°K (D) 1.75 kJ/°K (E) 2.25 kJ/°K (F) **1.57 kJ/°K** (G) 0.75 kJ/°K (H) 1.10 kJ/°K (I) 1.00 kJ/°K (J) 1.40 kJ/°K

**Golden Answer:** F

Base Model (Ouro-1.4B)	LoopRPT (Ours)
<p><i>Full Reasoning:</i>                      The change in entropy for a polytropic process is given by <math>\Delta S = nC_p \ln(T_2/T_1) - nR \ln(P_2/P_1)</math>. For air, <math>C_p = 1.005</math> kJ/kg·K and <math>R = 0.287</math> kJ/kg·K. Using the polytropic relation <math>P_1 V_1^n = P_2 V_2^n</math>, we find <math>V_2/V_1 = (P_1/P_2)^{1/n} \approx 0.554</math>. The temperature ratio <math>T_2/T_1 = (P_2/P_1)^{(n-1)/n} = (500/100)^{(1.56/2.56)} \approx 1.25</math>. Substituting into the entropy formula, <math>\Delta S \approx 3 \times 1.005 \times \ln(1.25) - 3 \times 0.287 \times \ln(5) \approx</math> <b>0.75 kJ/°K</b>.</p> <p><b>Conclusion:</b> The answer is (G) ✗</p>	<p><i>Full Reasoning:</i>                      The change in entropy is given by <math>\Delta S = mC_p \ln\left(\frac{T_2}{T_1}\right) - mR \ln\left(\frac{P_2}{P_1}\right)</math>. For an ideal gas, <math>C_p = \frac{nR}{n-1}</math> and <math>R</math> is the gas constant. Using the polytropic relation <math>P_1 V_1^n = P_2 V_2^n</math>, we find <math>T_2 = T_1 \left(\frac{P_2}{P_1}\right)^{\frac{n-1}{n}}</math>. <b>Substituting the given values, <math>T_2 = 300 \cdot \left(\frac{500}{100}\right)^{\frac{2.56-1}{2.56}} = 300 \cdot 5^{0.6094} \approx 799.6</math> K.</b> Then, <math>\Delta S = m \left[ c_p \ln\left(\frac{T_2}{T_1}\right) - R \ln\left(\frac{P_2}{P_1}\right) \right]</math>. <b>Calculating each term, <math>\Delta S = 3 \cdot \left[ 1.005 \ln\left(\frac{799.6}{300}\right) - 0.287 \ln(5) \right] \approx 1.57</math> kJ/K.</b></p> <p><b>Conclusion:</b> The answer is (F) ✓</p>

**Case 2: Biology (Thermoregulation)**

**Question:** Which of the following would maintain a constant body temperature in spite of changes in the environmental temperature: frog, robin, fish, dog, or lizard?

**Options:** (A) Robin, Lizard (B) Frog, Fish (C) Lizard, Frog (D) Fish, Dog (E) Fish, Lizard (F) Dog, Frog (G) Lizard, Fish (H) Frog, Robin (I) Dog, Lizard (J) **Robin, Dog**

**Golden Answer:** J

Base Model (Ouro-1.4B)	LoopRPT (Ours)
<p><i>Full Reasoning:</i>                      The correct answer is (A) Robin, Lizard. <b>Birds and reptiles are ectotherms</b>, meaning they rely on external sources of heat to maintain their body temperature. Frogs and fish are also ectotherms, but they are not included in the correct answer. Dogs are endotherms, meaning they can regulate their body temperature internally.</p> <p><b>Conclusion:</b> The answer is (A) ✗</p>	<p><i>Full Reasoning:</i>                      The correct answer is (J). <b>Dogs and robins are endothermic</b>, meaning they can maintain a constant body temperature in spite of changes in the environmental temperature. <b>Frogs, fish, and lizards are ectothermic</b>, meaning they cannot maintain a constant body temperature in spite of changes in the environmental temperature.</p> <p><b>Conclusion:</b> The answer is (J) ✓</p>

**Case 3: Computer Science (Discrete Logic)**

**Question:** Which of the following expressions evaluates to true if the person is old enough to drive ( $\geq 16$ ) but not old enough to vote ( $< 18$ )?

I. (age  $\geq 16$ ) AND (age  $\leq 18$ ) II. (age  $\geq 16$ ) AND (NOT(age  $\geq 18$ )) III. (age  $< 18$ ) AND (NOT(age  $< 16$ ))

**Options:** (A) II only (B) I and II only (C) I and III only (D) **II and III only**

**Golden Answer:** D

Base Model (Ouro-1.4B)	LoopRPT (Ours)
<p><i>Full Reasoning:</i>                      The correct answer is II only. The expression (age <math>\geq 16</math>) AND (NOT(age <math>\geq 18</math>)) evaluates to true if the person is at least 16 years old but not at least 18 years old... <b>The other expressions do not correctly represent the conditions.</b></p> <p><b>Conclusion:</b> The answer is (A) ✗</p>	<p><i>Full Reasoning:</i>                      The correct answer is (D). The first expression evaluates to true if the person is 16 or 17 years old, but it also evaluates to true if the person is 18 or older... The second expression evaluates to true if the person is 16 or 17 years old... <b>The third expression evaluates to true if the person is 16 or 17 years old, which is also what we want.</b></p> <p><b>Conclusion:</b> The answer is (D) ✓</p>

Figure 10. Comparative case study on general tasks (MMLU-Pro). LoopRPT successfully identifies implicit logical equivalences (Case 3) and maintains factual consistency in biological classification (Case 2), whereas the base model exhibits knowledge hallucinations or incomplete reasoning.

Case Analysis on Mathematical Tasks (GSM8K)	
<b>Case 1: Scheduling and Time Management</b>	
<b>Question:</b> Doctor Jones is spending nine hours at the clinic. He has to do rounds to check on inpatients (20 min/inpatient) and has ten appointments (30 min each). How many hours will he have left if he has 9 inpatients?	
<b>Golden Answer: 1</b>	
Base Model (Ouro-1.4B)	LoopRPT (Ours)
<p><i>Full Reasoning:</i>                      Doctor Jones is spending 9 hours at the clinic. He has to do rounds to check on inpatients, which takes 20 minutes per inpatient. He has 10 appointments, which take 30 minutes each. <b>So in total, he spends <math>20 * 10 + 30 * 10 = 200 + 300 = 500</math> minutes.</b> Converting minutes to hours, <math>500 / 60 = 8.33</math> hours. So he has <math>9 - 8.33 = 0.67</math> hours left.</p> <p><b>Conclusion:</b> The answer is 0.67 ✗</p>	<p><i>Full Reasoning:</i>                      Doctor Jones is spending 9 hours at the clinic. <b>He has 9 inpatients at the clinic. So he spends <math>20 * 9 = 180</math> minutes doing rounds.</b> He has 10 appointments, which take 30 minutes each. So he spends <math>30 * 10 = 300</math> minutes on appointments. <b>In total, he spends <math>180 + 300 = 480</math> minutes.</b> 9 hours is 540 minutes. So he has <math>540 - 480 = 60</math> minutes left (1 hour).</p> <p><b>Conclusion:</b> The answer is 1 ✓</p>
<b>Case 2: Multi-Agent Finance</b>	
<b>Question:</b> Maggie spent a quarter of her money, while Riza spent one-third of her money. They each had \$60. How much money do the two of them have left?	
<b>Golden Answer: 85</b>	
Base Model (Ouro-1.4B)	LoopRPT (Ours)
<p><i>Full Reasoning:</i>                      Maggie spent <math>1/4 * 60 = 15</math>. Riza spent <math>1/3 * 60 = 20</math>. So in total they spent <math>15 + 20 = 35</math>. <b>So they had <math>60 - 35 = 25</math>.</b></p> <p><b>Conclusion:</b> The answer is 25 ✗</p>	<p><i>Full Reasoning:</i>                      Maggie spent <math>1/4 * 60 = 15</math>. Riza spent <math>1/3 * 60 = 20</math>. Together, they spent <math>15 + 20 = 35</math>. <b>They had <math>60 + 60 = 120</math>. So they have <math>120 - 35 = 85</math> left.</b></p> <p><b>Conclusion:</b> The answer is 85 ✓</p>
<b>Case 3: Fractional Multi-step Calculation</b>	
<b>Question:</b> John has 8 classes (40 min each) for 5 days. He spends 1/16 of his weekly minutes each on Saturday and Sunday as extra time. How many hours a week does he spend learning?	
<b>Golden Answer: 30</b>	
Base Model (Ouro-1.4B)	LoopRPT (Ours)
<p><i>Full Reasoning:</i>                      Total class time is <math>8 * 40 * 5 = 1600</math> minutes. He spends 1/16 of his weekly minutes on Saturday and Sunday. <b>So in total he spends <math>1600 * 1/16 = 100</math> minutes.</b> So in total he spends <math>1600 + 100 = 1700</math> minutes (28.33 hours).</p> <p><b>Conclusion:</b> The answer is 28.33 ✗</p>	<p><i>Full Reasoning:</i>                      Total class time is <math>8 * 40 * 5 = 1600</math> minutes. <b>He then spends <math>1600 / 16 = 100</math> minutes each on Saturday and Sunday. So he spends <math>1600 + 100 + 100 = 1800</math> minutes in total.</b> 1800 minutes is 30 hours.</p> <p><b>Conclusion:</b> The answer is 30 ✓</p>

Figure 11. Comparison of GSM8K mathematical reasoning. Base model (Ouro-1.4B) frequently makes "set-neglect" errors (Case 2, 3) or hallucinations in variable mapping (Case 1), whereas LoopRPT correctly iterates through multi-step logic constraints.

Case Analysis on Coding Tasks (MBPP & HumanEval)	
<p><b>Case 1: MBPP (Mathematical Sequence)</b>  <b>Question:</b> Write a function to find the nth octagonal number. (Assertion: <code>is_octagonal(5) == 65</code>)  <b>Golden Answer:</b> <code>return 3 * n * n - 2 * n</code></p>	
Base Model (Ouro-1.4B)	LoopRPT (Ours)
<p><i>Generated Code:</i></p> <pre>def is_octagonal(n):     """Returns True if n is octagonal..."""     return n == (n * (3 * n - 1)) // 2</pre> <p><b>Analysis:</b> Confuses "nth number" request with "check property" and hallucinates pentagonal formula.  <b>Conclusion:</b> Functional Failure ✗</p>	<p><i>Generated Code:</i></p> <pre>def is_octagonal(n):     """Returns the n-th octagonal number."""     return 3 * n * n - 2 * n</pre> <p><b>Analysis:</b> Correctly identifies the task and provides the exact octagonal sequence formula.  <b>Conclusion:</b> Correct Generation ✓</p>
<p><b>Case 2: HumanEval (String Manipulation)</b>  <b>Question:</b> Find the shortest palindrome that begins with a supplied string by reverse-prefixing.  <b>Golden Answer:</b> Iteratively find longest palindromic suffix and append reverse prefix.</p>	
Base Model (Ouro-1.4B)	LoopRPT (Ours)
<p><i>Key Implementation:</i></p> <pre>for i in range(len(string), 0, -1):     if is_palindrome(string[-i:]):         break return string + string[:i-1][::-1]</pre> <p><b>Analysis:</b> Off-by-one error in indexing (i-1) leads to incorrect palindrome completion.  <b>Conclusion:</b> Logic Error ✗</p>	<p><i>Key Implementation:</i></p> <pre>for i in range(n):     if is_palindrome(string[i:]):         return string + string[:i][::-1]</pre> <p><b>Analysis:</b> Accurately iterates through split points to find the optimal palindromic suffix.  <b>Conclusion:</b> Correct Generation ✓</p>
<p><b>Case 3: HumanEval (Cyclic Array Order)</b>  <b>Question:</b> Determine if an array can be sorted by performing any number of right shifts.</p>	
Base Model (Ouro-1.4B)	LoopRPT (Ours)
<p><i>Key Implementation:</i></p> <pre>for i in range(n):     if arr[i] &gt; arr[(i + 1) % n]:         return False return True</pre> <p><b>Analysis:</b> Incorrectly implements a strict sorted check, failing for valid cyclic shifts.  <b>Conclusion:</b> Logic Error ✗</p>	<p><i>Key Implementation:</i></p> <pre>sorted_arr = sorted(arr) for i in range(len(arr)):     if arr == sorted_arr[i:] + sorted_arr[:i]:         return True</pre> <p><b>Analysis:</b> Correctly uses a cyclic comparison loop to verify all possible shift states.  <b>Conclusion:</b> Correct Generation ✓</p>

Figure 12. **Code generation comparison.** Base model (Ouro-1.4B) fails on boundary conditions and algorithmic interpretation, while LoopRPT demonstrates superior adherence to task constraints.

---

**Algorithm 1** Phase I: Dense Step-wise Reward Table Construction with RPT Token Filtering
 

---

**Require:** Batch  $\{x_{0:S}\}$  with valid-token mask  $m \in \{0, 1\}^{B \times (S-1)}$  (aligned to next-token positions); student  $\theta$ ; EMA teacher  $\bar{\theta}$ ; max steps  $K$ ; exit threshold  $\tau$ ; top-ratio  $\rho$ ;  $\lambda_{\text{base}}, \lambda_{\text{scale}}$ ; constant  $\varepsilon$ .

**Ensure:** RPT mask  $m_{\text{RPT}}$ ; reward table  $\{R_t(k)\}_{k=1}^K$ ; step advantage  $\{A_{b,t}(k)\}_{k=1}^K$ .

- 1: **Teacher forward (for hard-token selection and reference quantities)**
- 2: Run teacher LoopLM for  $K$  steps to obtain last-step logits  $\bar{z}_t^{(K)}$  and gate logits  $\{\bar{a}_t^{(k)}\}_{k=1}^K$  at each next-token position  $t$ .
- 3: Compute last-step entropy  $H_t^{\text{last}} = -\sum_{v \in V} \bar{p}_t(v) \log \bar{p}_t(v)$  where  $\bar{p}_t = \text{Softmax}(\bar{z}_t^{(K)})$ .
- 4: **RPT hard-token filtering (top- $\rho$  entropy on valid positions)**
- 5: **for** each example  $i$  in the batch **do**
- 6:      $q_i \leftarrow \text{Quantile}(\{H_{i,t}^{\text{last}} : m_{i,t} = 1\}, 1 - \rho)$
- 7:      $m_{\text{RPT},i,t} \leftarrow \mathbb{I}[H_{i,t}^{\text{last}} > q_i]$
- 8: **end for**
- 9:  $m \leftarrow m \odot m_{\text{RPT}}$
- 10: **Reference step**  $t_{\text{ref}}$  **and dynamic baseline**  $b_{\text{ref}}$
- 11: Compute teacher exit distribution  $\pi_{\bar{\theta}}(k)$  via Eq. (2–3) from  $\{\bar{a}_t^{(k)}\}$  and its CDF  $\Pi_{\bar{\theta}}(k) = \sum_{j \leq k} \pi_{\bar{\theta}}(j)$ .
- 12:  $t_{\text{ref}} \leftarrow \min\{k : \Pi_{\bar{\theta}}(k) \geq \tau\}$  (use  $K$  if never exceeded).
- 13: Compute teacher per-step gold log-prob  $\ell_{\bar{\theta}}^{(k)}(t) = \log p_{\bar{\theta}}(x_t | x_{<t}, \bar{h}_t^{(k)})$ .
- 14: Set  $b_{\text{ref}}(t) \leftarrow \ell_{\bar{\theta}}^{(t_{\text{ref}})}(t)$  ▷ Eq. 5
- 15: **Difficulty-aware time penalty weight**  $\lambda_t$
- 16: Compute teacher entropy at the reference step  $H_t^{\text{ref}}$  (from teacher distribution at  $t_{\text{ref}}$ ).
- 17:  $d_t \leftarrow \text{Clamp}(H_t^{\text{ref}} / \log |V|, 0, 1)$ ,  $\lambda_t \leftarrow \lambda_{\text{base}} (1 + \lambda_{\text{scale}} (1 - d_t))$  ▷ Eq. 8
- 18: **Student deterministic pass for step-wise rewards**
- 19: Run student without noise to obtain  $\ell_{\theta}^{(k)}(t) = \log p_{\theta}(x_t | x_{<t}, h_t^{(k)})$  for  $k = 1, \dots, K$ .
- 20: **for**  $k = 1, \dots, K$  **do**
- 21:      $\Delta_{\text{acc},t}(k) \leftarrow \ell_{\theta}^{(k)}(t) - b_{\text{ref}}(t)$  ▷ Eq. 6
- 22:      $C_t(k) \leftarrow \lambda_t (k - t_{\text{ref}})$  ▷ Eq. 7
- 23:      $R_t(k) \leftarrow \Delta_{\text{acc},t}(k) - C_t(k)$  ▷ Eq. 9
- 24: **end for**
- 25: **Step advantage for representation learning**
- 26:  $\mu_{R,t} \leftarrow \frac{1}{K} \sum_{j=1}^K R_t(j)$ ,  $\sigma_{R,t} \leftarrow \sqrt{\frac{1}{K} \sum_{j=1}^K (R_t(j) - \mu_{R,t})^2}$
- 27: **for**  $k = 1, \dots, K$  **do**
- 28:      $A_{b,t}(k) \leftarrow \frac{R_t(k) - \mu_{R,t}}{\sigma_{R,t} + \varepsilon}$  ▷ Eq. 10
- 29: **end for**
- 30: **return**  $(m_{\text{RPT}}, \{R_t(k)\}_{k=1}^K, \{A_{b,t}(k)\}_{k=1}^K)$  on positions where  $m = 1$ .

---

---

**Algorithm 2** Phase II: Noisy Rollout Policy Gradient + Step-Weighted Next-Token Training
 

---

**Require:** Batch  $\{x_{0:S}\}$  with effective mask  $m$  (after Alg. 1); student  $\theta$ , EMA teacher  $\bar{\theta}$ ; max steps  $K$ , threshold  $\tau$ ; reference quantities from Phase I:  $t_{\text{ref}}$ ,  $b_{\text{ref}}(t)$ ,  $\lambda_t$ , and  $A_{b,t}(k)$ ; rollouts  $G$ , noise scale  $\sigma$ ; loss weights  $\alpha, \beta, \gamma, \delta$ ; constant  $\varepsilon$ .

**Ensure:** Updated  $\theta$  and EMA teacher  $\bar{\theta}$ .

- 1: **Deterministic student pass (for  $\pi_\theta$  and step-weighted NTP)**
  - 2: Run student without noise to obtain gate logits  $\{a_t^{(k)}\}_{k=1}^K$  and per-step gold log-probs  $\ell_\theta^{(k)}(t)$ .
  - 3: Compute exit distribution  $\pi_\theta(k)$  via Eq. (2–3).
  - 4: **for**  $k = 1, \dots, K$  **do**
  - 5:      $w_t(k) \leftarrow \pi_\theta(k) \left(1 + \text{ReLU}(A_{b,t}(k))\right)$  ▷ Eq. 15
  - 6: **end for**
  - 7:  $L_{\text{rep}} \leftarrow -\sum_{k=1}^K w_t(k) \ell_\theta^{(k)}(t)$  ▷ Eq. 14  
(Applied only on positions where  $m = 1$ ; sums/means are over those positions.)
  - 8: **Entropy regularization on exit distribution**
  - 9:  $L_{\text{ent}} \leftarrow -\mathbb{E} \left[ \sum_{k=1}^K \pi_\theta(k) \log \pi_\theta(k) \right]$ .
  - 10: **Noisy latent rollouts with reward regain (on-policy reward recomputation)**
  - 11: **for**  $g = 1, \dots, G$  **do**
  - 12:     Run a noisy recurrence (Eq. 11) to obtain noisy states  $\{h_{t,g}^{(k)}\}_{k=1}^K$  and rollout gates  $\{a_{t,g}^{(k)}\}_{k=1}^K$ .
  - 13:     Compute rollout exit distribution  $\pi_\theta^{(g)}(k)$  from  $\{a_{t,g}^{(k)}\}$ .
  - 14:     Recompute per-step gold log-probs on rollout states:  $\ell_{\theta,g}^{(k)}(t) = \log p_\theta(x_t \mid x_{<t}; h_{t,g}^{(k)})$ .
  - 15:     **for**  $k = 1, \dots, K$  **do**
  - 16:          $\Delta_{\text{acc},t}^{(g)}(k) \leftarrow \ell_{\theta,g}^{(k)}(t) - b_{\text{ref}}(t)$
  - 17:          $C_t(k) \leftarrow \lambda_t (k - t_{\text{ref}})$
  - 18:          $R_t^{(g)}(k) \leftarrow \Delta_{\text{acc},t}^{(g)}(k) - C_t(k)$
  - 19:     **end for**
  - 20:     Sample exit step  $t^{(g)} \sim \pi_\theta^{(g)}(\cdot)$  and set rollout reward  $r^{(g)} \leftarrow R_t^{(g)}(t^{(g)})$ .
  - 21: **end for**
  - 22: **Group-normalized rollout advantage and policy gradient**
  - 23:  $A^{(g)} \leftarrow \frac{r^{(g)} - \text{mean}_g[r^{(g)}]}{\text{std}_g[r^{(g)}] + \varepsilon}$  ▷ Eq. 12
  - 24:  $L_{\text{PG}} \leftarrow -\mathbb{E}_g \left[ A^{(g)} \log \pi_\theta^{(g)}(t^{(g)}) \right]$  ▷ Eq. 13
  - 25: **Rollout KL regularization (K3 surrogate, rollout aggregation)**
  - 26: Compute teacher per-step gold log-probs  $\ell_{\bar{\theta}}^{(k)}(t)$  on the same rollout-evaluated tokens/steps.
  - 27: **for**  $k = 1, \dots, K$  **do**
  - 28:      $\Delta^{(k)} \leftarrow \ell_{\bar{\theta}}^{(k)}(t) - \ell_{\theta,g}^{(k)}(t)$  ▷ Eq. 40
  - 29:      $u^{(k)} \leftarrow \exp(\Delta^{(k)})$ ,  $K3(k) \leftarrow u^{(k)} - \Delta^{(k)} - 1$  ▷ Eq. 41
  - 30: **end for**
  - 31: Let  $m_G$  be the rollout mask indicating the positions/steps evaluated in the rollout pass.
  - 32:  $L_{\text{KL}} \leftarrow \frac{\sum_{k=1}^K K3(k) \odot m_G}{\sum m_G + \varepsilon}$  ▷ Eq. 42
  - 33: **Total objective and updates**
  - 34:  $L \leftarrow \alpha L_{\text{PG}} + \beta L_{\text{rep}} + \gamma L_{\text{ent}} + \delta L_{\text{KL}}$  ▷ Eq. 16
  - 35: Update  $\theta$  by one gradient step on  $L$ ; update EMA teacher  $\bar{\theta} \leftarrow \text{EMA}(\bar{\theta}, \theta)$ .
-